# Rapid, population-wide declines in stem cell number and activity during reproductive aging in *C. elegans*

**Authors:** Zuzana Kocsisova[1, 2], Kerry Kornfeld*[1], & Tim Schedl*[2]

*These authors contributed equally.

**Affiliations:**
1, Department of Developmental Biology, Washington University School of Medicine, St. Louis, Missouri, USA
2, Department of Genetics, Washington University School of Medicine, St. Louis, Missouri, USA

**Institutional Address:** 660 S. Euclid Ave, St. Louis, MO 63108

**Email Addresses:** zuzana@wustl.edu, ts@wustl.edu, kornfeld@wustl.edu

**Categories:** Development- Germline Development; Physiology- Aging and Stress

**Key Words**: Germline, Reproductive Aging, Caenorhabditis, Stem Cells, Notch, Cell Cycle, Endomitotic Oocytes, Meiotic development

© 2019. Published by The Company of Biologists Ltd.

Development • Accepted manuscript

## Summary Statement:

Age-related reproductive decline in *C. elegans* results from sporadic defects in a small fraction of animals, but primarily results from population-wide processes affecting stem cell number, Notch signaling, cell cycle timing, and meiotic entry and progression in all animals.


## Abstract:

*C. elegans* hermaphrodites display dramatic age-related decline of reproduction early in life while somatic functions are still robust. To understand reproductive aging, we analyzed the assembly line of oocyte production that generates fertilized eggs. Aging germlines displayed both sporadic and population-wide changes. A small fraction of aging animals displayed endomitotic oocytes in the germline and other defects. By contrast, all animals displayed age-related decreases in germline size and function. As early as day 3 of adulthood, animals displayed fewer stem cells and a slower cell cycle, which combine to substantially decrease progenitor zone output. The *C. elegans* germline is the only adult tissue that contains stem cells, allowing the analysis of stem cells in aging. To investigate the mechanism of the decrease in stem cell number, we analyzed the Notch signaling pathway. The Notch effectors LST-1 and SYGL-1 displayed age-related decreases in expression domains, suggesting a role for Notch signaling in germline aging. The results indicate that while sporadic defects account for the sterility of some animals, population-wide changes account for the overall pattern of reproductive aging.


Development • Accepted manuscript

## Introduction

Aging is characterized by progressive degenerative changes of tissue structure and function that impair physiology and ultimately lead to death. A critical first step in understanding these changes is characterizing age-related changes in wild-type tissues, which constitutes the starting point for uncovering genes and pathways that modulate age-related decline. Most aging research focuses on somatic aging and lifespan. By contrast, much less is understood about aging of the reproductive system. Reproductive aging, which we define as the progressive, age-related decline of the ability of the reproductive system to produce offspring, is important for human health, since infertility is an increasing concern for women who wait until middle age to start families. The *Caenhorbditis elegans* hermaphrodite is an important model because the ability to produce oocytes displays rapid age-related decline and ceases entirely while the animals are all still alive, moving, and feeding (Hughes et al., 2007). Furthermore, the *C. elegans* germline is the only adult tissue that contains stem cells, allowing study of stem cells in aging (Luo and Murphy, 2011; Pazdernik and Schedl, 2013). Extensive studies of reproductive function have been conducted in young adults, where germline stem cells differentiate and mature in a linear assembly line-like pattern as they progress away from the somatic distal tip cell (DTC) toward the spermatheca and uterus over the course of about two days (**Fig.1C**). The ~20 cell-diameter long region of the germline that is capped by the DTC niche is called the progenitor zone (PZ); it includes the mitotically cycling germline stem cells, progenitor cells, and meiotic S-phase cells, and is followed by stages of meiotic prophase and gametogenesis (Crittenden et al., 2006; Fox et al., 2011; Hansen and Schedl, 2013; Kimble and Seidel, 2013; Pazdernik and Schedl, 2013). At the proximal end, oocytes mature, are ovulated and fertilized, and begin embryogenesis in the uterus (Hirsh et al., 1976; Pazdernik and Schedl, 2013). Measures of egg laying are a convenient surrogate for measures of ovulation, because ~100% of ovulations in sperm-replete animals result in live progeny (McCarter et al., 1999).

While the age-related decline of reproductive output has been well-documented for many years (de la Guardia et al., 2016; Garigan et al., 2002; Hughes et al., 2007; Hughes et al., 2011), it remains unclear which processes in the assembly line of oocyte production begin and sustain this decline. Previous studies have examined aging mechanisms in sperm-depleted and/or older animals (Luo et al., 2010; Narbonne et al., 2015; Qin and Hubbard, 2015). To begin to understand why the germline declines early in adult life, we applied state-of-the-art techniques to characterize the cellular and molecular changes that underlie age-related functional decline using sperm-replete animals before and during the decline in reproduction. Here, we report that aging germlines displayed both sporadic and population-wide changes. A small fraction of aging animals displayed endomitotic oocytes in the germline and a shifted DTC nucleus; longitudinal studies indicate that the sporadic endomitotic oocyte phenotype contributed to reduced progeny production, but only in a subset of aging animals. By contrast, there was a population–wide decrease in germline and PZ size during aging. The PZ mitotic cell cycle slowed, the number of germ cells entering meiosis decreased, and the rate of meiotic prophase progression decreased. The domain of expression of GLP-1/Notch signaling effectors SYGL-1 and LST-1 decreased, indicating that stem cell number declined and suggesting there was an age-related downregulation of GLP-1/Notch signaling. These population-wide changes in the distal germline began as early as day 3 of adulthood, when reproductive output was at its peak. An

Development • Accepted manuscript

important theoretical issue in aging research is the role of sporadic, "stochastic' damage as a cause of age-related degenerative change versus the role of population-wide, "programmed" decline. For example, Herndon et al. (2002) reported on the heterogeneity among aging individuals and described the stochastic nature of somatic aging. Our results highlight the importance of population–wide changes in driving age-related decline of germline function and suggest that decreased number and activity of germline stem cells may be a root cause of reproductive aging.

Development • Accepted manuscript

## Results:

### Rapid, population-wide reproductive aging preceded somatic aging

An age-related decline in progeny production occurs in both self-fertile and mated hermaphrodites (Hughes et al., 2007). Wild-type hermaphrodites produced on average ~150 progeny in 24 hours at the peak of their reproductive ability on adult day 2 (**Fig.1A**). In self-fertile hermaphrodites, progeny number decreased to ~60 by day 3 (two-fold decrease), to ~8 by day 5 (twenty-fold decrease), and was negligible after that. This rapid decline was due to sperm depletion, complicating interpretation of these data relative to reproductive aging. To monitor reproductive aging without the confounding variable of sperm depletion (Angeles-Albores et al., 2017), we analyzed mated hermaphrodites. Mating for 24 hours beginning at the L4 stage provides sufficient sperm to avoid sperm depletion, evidenced by production of male progeny until the cessation of reproduction and no increase in brood size after re-mating at day 5 (Cinquin et al., 2016; Hughes et al., 2007; Pickett et al., 2013; Ward and Carrel, 1979). The presence of sperm was confirmed by immunostaining for major sperm protein when possible, and sperm-depleted animals were excluded from analyses. In mated hermaphrodites, progeny number is increased and the reproductive span is extended compared to self-fertile animals. Nevertheless, progeny production declines to ~40 by day 5 (four-fold decrease) and to ~12 by day 7 (fourteen-fold decrease) due to aging of the reproductive tract, consistent with previous findings (Hughes et al., 2007). In contrast to the rapid decline of progeny production, the decline of survival probability was slower; 100% of mated hermaphrodites were alive at day 10 and half remained alive until day 16 (**Fig.1A**). Thus, the age-related decline of progeny production occurs in animals with relatively healthy somatic tissue.

### Endomitotic oocytes were a sporadic, low frequency, age-related defect that negatively affected reproduction

To investigate the basis for reproductive aging in mated hermaphrodites, we analyzed the morphology of dissected germlines in day 1, 3 and 5 adults. The ability to withstand dissection is unlikely to affect these comparisons, because gonads dissect reliably at these ages. DAPI staining was used to analyze nuclear morphology, and WAPL-1 antibody staining was used to measure the size of the PZ and the position of the DTC and somatic gonad nuclei (**Fig.S1**). Some abnormalities were observed at such a low frequency (<2% of germlines) that they could not be effectively studied with our sample size. These included premature meiotic entry of all PZ cells (Glp phenotype), short and narrow PZ, enlarged PZ nuclei, ectopic proliferation, and gaps and oocyte-like formations in the middle of the pachytene region (**Fig.S2**). Two abnormalities were observed at a low but consistent frequency that supported statistical analysis: the presence of endomitotic oocytes and a shifted DTC nucleus.

Endomitotic oocytes within the proximal gonad arm result from miscoordination of meiotic maturation and ovulation and can be visualized with DAPI staining (**Fig.2D**). Mutations of at least 21 genes are known to result in endomitotic oocytes (Greenstein, 2005; Iwasaki et al., 1996; McCarter et al., 1997; Wormbase WS260, 2017). Endomitotic oocytes can negatively affect reproduction, since several endomitotic oocytes in a gonad block productive maturation and ovulation. In mated hermaphrodites, endomitotic oocytes were extremely rare in day 1 adults. There was an age-related increase in frequency; about 5% of day 3 adults displayed single

Development • Accepted manuscript

endomitotic oocytes, usually in only one gonad arm, positioned distal to the spermatheca and not in the uterus (**Fig.2A**). At least 9% of germlines of day 5 adults displayed endomitotic oocytes, and affected animals typically displayed multiple endomitotic oocytes with large nuclei, often in both gonad arms.

To investigate the model that endomitotic oocytes cause an age-related decrease in progeny production, we performed a longitudinal analysis. Progeny production by mated wild-type hermaphrodites is quite variable in the 24 hours between days 4 and 5, averaging 32 +/- 18 and ranging from 0 to 108 (**Fig.2B**). We measured progeny production in this interval for 186 hermaphrodites, then sacrificed the animals and measured endomitotic oocytes. The subpopulation with the lowest progeny production exhibited significantly more endomitotic germlines than the other subpopulations (**Fig.2C**). There was no significant correlation between the least-fertile subpopulation and distal germline phenotypes (**Fig.S3E,F**). The strong correlation between the presence of endomitotic oocytes and low progeny production suggests these two processes are causally linked.

The somatic DTC caps the end of the germline and intercalates between the distal germ cells. The DTC provides the niche for the germline stem cells by expressing LAG-2 (delta ligand) that is received by GLP-1 (Notch receptor) on the germline stem cells (Greenwald and Kovall, 2013; Kimble and Seidel, 2013; Kimble and Ward, 1988; Pazdernik and Schedl, 2013; Pepper et al., 2003). To monitor age-related changes, we determined the position of the DTC nucleus relative to the distal end of the germline (**Fig.2E**). In day 1 adults, the DTC nucleus was always positioned within 3 cell diameters (c.d.) of the end of the germline. Day 3 and 5 adults displayed a shift of 5 c.d. or more in 7% and 17% of germlines, respectively (**Fig.2F,G;Fig.S3B**). To analyze the functional consequences of the shifted DTC, we used a longitudinal approach to determine the correlation with progeny production between days 4 and 5. Although the least-fertile subpopulation displayed a higher extent of shifted DTC nucleus, the trend was not statistically significant with this sample size (**Fig.S3E**). Additionally, the shifted DTC nucleus and endomitotic oocyte phenotypes were not correlated (**Fig.2H,I; Fig.S3C,D**). These results document an age-related increase in the frequency of a shifted DTC but do not rigorously establish the functional consequences of this anatomical change, and it is possible that it does not negatively influence reproduction.

If endomitotic oocytes or shifted DTC nuclei are caused by systemic factors, then the two gonad arms of an individual are predicted to display similar behavior. By contrast, if these abnormalities result from anatomically local causes, then the two gonad arms in an individual are predicted to behave independently. To investigate these possibilities, we took advantage of the subset of animals in which both germlines were visible after dissection and compared within-pair variation to between-pair variation using an intraclass correlation analysis. There was no significant correlation in the degree of DTC nucleus shift within a pair of germlines in the same animal (**Fig.S3G-I**). Thus, the shifted DTC nucleus appears to result from local rather than systemic conditions. By contrast, if one gonad arm displayed endomitotic oocytes, then the other arm was also more likely to display this defect, indicating there may be systemic conditions that promote this defect (**Fig.S3A**).

Development • Accepted manuscript

**Population-wide, age-related decline in the size of the germline and progenitor zone**

The majority of day 5 adults displayed neither endomitotic oocytes nor a shifted DTC nucleus, yet all these animals produced far fewer progeny than young adults. To explain the population-wide decline in progeny production, we searched for age-related changes in the germline that affect all animals. To measure germline size, we counted the number of cell diameters from the distal tip to the loop (distal portion of the germline) or the distance in micrometers from the distal tip to the spermatheca (entire germline). Both measurements revealed a significant decrease in overall size at days 3 and 5 (**Fig.3B,C**). The size of the PZ measured in cell diameters or total number of cells displayed a significant and progressive decrease (**Fig.3A,D,E**). The age-related changes identified in this cross sectional analysis appear to affect essentially the entire population, albeit within a normal distribution (**Fig.3B-F**).

If the decreased size of the PZ is caused by systemic factors, then a similar decrease is predicted to occur in both gonad arms of an individual. Indeed, a significant within-pair correlation of PZ size in day 3 and 5 adults was observed (**Fig.S4A-C**). The low relative variance within pairs of day 3 and 5 germlines is consistent with an age-related systemic process that affects both gonad arms in an individual animal.

To investigate the relationship between the DTC nucleus position and the size of the PZ, we analyzed the correlation between these features. Overall, the position of the DTC nucleus did not explain the decrease in the size of the PZ, indicating these two age-related changes do not share a common cause (**Fig.S4D-F**). Day 3 hermaphrodites that were self-fertile or mated to males displayed similar distal germline sizes and extents of the PZ, indicating male exposure did not cause these age-related changes (**Fig.S5**).

**The duration of the mitotic cell cycle displayed population-wide, age-related increase.**

The reduction in size of the PZ may be the result of a decrease in the frequency of cell division and/or the size of the stem cell pool. To analyze the cell cycle, we measured multiple parameters that make it possible to calculate the overall duration of the cell cycle and the proportion of each phase (**Fig.1B,S1**). In day 1 adult hermaphrodites, the mitotic cell cycle takes 6.5-8 hours, germ cells do not undergo transit-amplifying divisions (Fox and Schedl, 2015), and quiescent cells are not observed (Crittenden et al., 2006). The cell cycle consists of the phases S, G2, and M, since the G1-phase is short or absent (Fox et al., 2011). To investigate age-related changes in the cell cycle, we measured the mean and maximum duration of the cell cycle in day 1, 3 and 5 adults.

To estimate the durations of cell cycle phases, we fed animals EdU continuously for 0.5, 4, 7, or 10 hours and dissected them immediately. A significant fraction of day 5 animals failed to label following a 0.5 hour EdU feed; the alternative method of soaking in EdU gave a similar result (see Methods; **Fig.S6**). Cinquin et al., (2016) reported a similar phenomenon. Some day 5 animals may have reduced ability to absorb and transport EdU. These animals were not informative about cell cycle duration and were excluded from data analysis.

The duration of G2 was estimated by analyzing the percent of cells in M-phase (pH3 immunoreactive) that were EdU-positive; these cells must have been in S-phase during the EdU pulse and then proceeded through G2 and entered M-phase at the time of dissection (**Fig.4A,B**). No M-phase cells were EdU-positive after a 0.5-hour pulse, indicating G2 was always more than 0.5 hours, whereas all M-phase cells were EdU-positive after a 10-hour pulse, indicating G2 was always less than 10 hours. Using all four data points, we estimated the median G2 duration as

Development • Accepted manuscript

~2.5, ~4.5 and ~4.9 hours in day 1, 3, and 5 animals, respectively. Thus, there was a significant ~100% increase in the duration of G2 between days 1 and 3.

The duration of G2+M+G1 was estimated from the percentage of all PZ cells (WAPL-1-immunoreactive) that were EdU-negative (**Fig.4C,D**). About 40% of cells were EdU-negative following a 0.5 hour pulse, indicating these cells were in G2+M+G1 during the entire pulse, whereas no cells were EdU-negative following a 10 hour pulse, indicating G2+M+G1 was always less than 10 hours. These data were used to calculate maximum duration of these three phases, and the 90$^{th}$ percentile duration was determined by interpolation. We estimated the 90$^{th}$ percentile G2+M+G1 duration as ~3.4, ~7.6, and ~7.4 hours in day 1, 3, and 5 animals, respectively. Thus, there was a significant ~100% increase in the duration of G2+M+G1 between days 1 and 3.

In principle, there are two explanations for the age-related increase in median and maximum cell cycle durations across the population of PZ cells at day 3: 1) in all cells the duration of all phases of the cell cycle increased proportionately or 2) in some cells one phase of the cell cycle increased disproportionately, similar to cell cycle arrest that occurs during germline starvation, sperm depletion, and during *Drosophila* germline aging (Angelo and Van Gilst, 2009; Kao et al., 2015; Narbonne et al., 2015; Seidel and Kimble, 2015). To distinguish these possibilities, we determined the fraction of cells in M-phase using anti-pH3 antibody (M-phase index, **Fig.4F, S7A,B,D**) and the fraction of cells in S-phase using a 0.5 hour pulse of EdU (S-phase index, **Fig 4E,G, S7C,E**). The M-phase index was approximately 2.5% in day 1, 3 and 5 animals, indicating there is not an age-related change in the fraction of cells in M-phase. Similarly, the S-phase index did not display an age-related change but was approximately 57% in day 1, 3 and 5 animals. These results indicate that adult germline stem cells do not become quiescent, at least up to day 3 of adulthood. These results indicate there is an age-related increase in cell cycle duration in all cells, whereas there is no age-related change in the proportion of cells in each cell cycle phase (**Fig.4H**).

**The rate of meiotic entry, a measure of the output of the progenitor zone, displayed population-wide, age-related decline.**

A critical factor in germline function is the rate at which cells exit the PZ and enter meiosis. We predicted the output of the PZ would decrease in day 3 and 5 adults as a functional consequence of a slower cell cycle and a smaller stem cell pool (see below). To measure the rate of meiotic entry, we exposed animals to EdU for 4, 7, or 10 hours and counted the number of EdU-positive cells in the meiotic region, defined as cells that displayed EdU signal but no WAPL-1 signal. These cells must have resided in the PZ at the beginning of the experiment to become EdU labeled and then entered the meiotic region by the end of the experiment to become WAPL-1-negative (**Fig.5A**).

The rate of meiotic entry was calculated as the slope of the regression using three data points (**Fig.5B**). Day 1 animals displayed 19.3 cells per hour entering meiosis, consistent with previous reports (Fox et al., 2011). Day 3 and 5 animals displayed a much lower rate, only ~4 and ~2 cells per hour entering meiosis, respectively. There was no significant correlation between the size of the PZ and the number of cells that entered meiosis in day 1, 3 and 5 animals (**Fig.S8**). Thus, the rate of meiotic entry displayed a dramatic age-related decrease of ~78% by day 3 and over 91% by day 5 (**Fig.5C**).

Development • Accepted manuscript

A large proportion of germ cells that enter meiosis in the adult function as nurse cells that provide essential constituents to growing oocytes but do not become oocytes, as they undergo apoptosis in late pachytene (Gumienny et al., 1999; Wolke et al., 2007). We estimate that 84% of day 1 cells that enter meiosis become nurse cells, similar to other estimates (see Methods; Agarwal et al., 2018). The number of nurse cells did not change significantly at day 3 (79%) and day 5 (85%).

**The assembly-line-like progression from the progenitor zone to oocytes displayed population-wide, age-related decline.**

The rate at which cells progress through meiotic prophase is an important aspect of germline function. To determine how this value changes during aging, we used an EdU pulse-chase technique similar to that reported by Jaramillo-Lambert *et al.* (2007). The "pulse" consisted of 4 hours feeding with EdU labeled bacteria, which marks the majority of PZ cells. The "chase" consisted of transferring animals to unlabeled bacteria for 48 hours, followed immediately by dissection. Cells labeled with EdU during the "pulse" retain this label during the "chase" as they progress through meiotic prophase and gametogenesis (**Fig.6A**). Thus, the most proximal labeled cells provide a measure of the distance travelled from the PZ in 48 hours. Because the distance is measured during a two-day interval, the rate is an average during days 1-3, 3-5, or 5-7. We analyzed the length of the germline, length of the PZ, and the position of the most-proximal cell of the population of EdU labeled cells (**Fig.6C, Fig.S9A-C**). In addition, the meiotic prophase substage (mid-pachytene, late pachytene, diplotene, or diakinesis) of the most proximal EdU positive cell was determined (**Fig.6D, S9D,E**).

The rate of progression through meiotic prophase decreased in day 3 and 5 compared to day 1. Starting with day 1 adults, after 48 hours the most proximal cell progressed ~52 c.d. (**Fig.6C**). It was most commonly in diplotene, with some in late pachytene and some in diakinesis (**Fig.6D, S9D,E**). Day 3 animals displayed significantly less movement and maturity after 48 hours. The most proximal cell progressed ~31 c.d., despite the entire germline decreasing in size, and was most commonly in late pachytene (**Fig.6C,D, S9D,E**). Day 5 adults were not significantly different compared to day 3 adults. Thus, the rate that cells move through meiotic prophase during days 3-5 was dramatically slower than the rate during days 1-3 (**Fig.6E**).

**Age-related changes in the distal germline have a delayed effect on progeny production.**

Our results document that the distal gonad displays striking age-related declines by day 3, but at this time progeny production is still at or near its peak. We reasoned that the changes in the distal gonad would have a delayed effect on progeny production that might not be apparent until about 2.5 days later, given the time necessary for germ cells to transit through the germline (**Fig.6**). Thus, progeny deposited into the environment at day 3 result from PZ cells on day 1 that transitioned into developing oocytes in the proximal arm of the germline. This model predicts that the number of developing oocytes would remain unchanged between days 1 and 3 but would decrease by day 5. To test this hypothesis, we counted the number of oocytes in diplotene and diakinesis in dissected DAPI-stained germlines. The number of oocytes was ~14 at days 1 and 3, but decreased significantly to ~9 at day 5 (**Fig.6B**). Thus, the effect on progeny production caused by the slowing cell cycle and shrinking size of the PZ at day 3 only appears about 2 days later.

Development • Accepted manuscript

**A population-wide, age-related decline in stem cell number and the domain of Notch signaling**

Our results document dramatic changes in the number and behavior of the PZ cells by days 3 and 5. To further investigate the mechanisms that promote these changes, we took a candidate approach by analyzing the Notch signaling pathway. The DTC expresses LAG-2 (Delta), which interacts with GLP-1(Notch) receptor on germ cells. Following GLP-1 cleavage, the intracellular domain translocates to the nucleus and interacts with LAG-1 to activate the transcription of Notch effector genes (Greenwald and Kovall, 2013; Kershner et al., 2014; Kimble and Ward, 1988; Lee et al., 2016; Pazdernik and Schedl, 2013; Pepper et al., 2003; Shin et al., 2017). Notch signaling is critical for the stem cell fate, since withdrawal of Notch signaling results in entry into meiosis. We hypothesized that an age-related decrease in GLP-1/Notch signaling contributes to age-related changes in stem cell fate specification. Two direct transcriptional targets of GLP-1 are the *sygl-1* and *lst-1* genes, which are redundantly necessary and each sufficient to promote germline stem cell fate and block differentiation (Kershner et al., 2014; Lee et al., 2016). To analyze *sygl-1* and *lst-1* expression, we engineered the FLAG epitope tag into the endogenous loci so that these genes express FLAG::SYGL-1 and LST-1::FLAG, respectively (**Fig.7A,E**).

To investigate whether the number of germline stem cells decreases with age, we used FLAG::SYGL-1. We interpret the SYGL-1 expression zone to approximate the stem cell pool, as genetic analysis indicates SYGL-1 is sufficient for the stem cell fate (Shin et al., 2017). Dissected germlines of day 1 adults displayed expression of FLAG::SYGL-1 in the cytoplasm of the most distal ~10 cell diameters of the germline; the FLAG::SYGL-1 region encompassed 81 +/- 14 cells. (**Fig.7B-D, S10C**). Day 3 adults displayed a significant ~1.4-fold decrease in the number of FLAG::SYGL-1 cells, and day 5 adults displayed a significant ~2-fold decrease (**Fig.7C,I**). The expression zone measured in cell diameters displayed a similar age-related decline (**Fig.7D**). Thus, the extent of SYGL-1 expression displayed age-related decline by day 3, indicating there is an age-related decline in the number of germline stem cells.

To investigate whether changes in GLP-1/Notch signaling are responsible for the age-related decrease in the size of the PZ, we used LST-1::FLAG. Dissected germlines of day 1 adults stained with anti-FLAG antibody displayed expression of LST-1::FLAG in the cytoplasm of the most distal ~5 cell diameters (**Fig.7F-H, S10A**), which corresponded well with the localization of *lst-1* pre-mRNA introns, and thus the region of Notch-mediated transcription (Lee et al., 2016). Consistent with this interpretation, when the DTC nucleus was shifted, the domain of LST-1::FLAG displayed a corresponding shift (**Fig.S10B**). The LST-1::FLAG region encompassed 38 +/-10 cells at day 1 (**Fig.7G**). Day 3 adults displayed a significant ~1.4-fold decrease in the number of LST-1::FLAG cells, and day 5 adults displayed a further significant ~2.2-fold decrease (**Fig.7G,I**). The expression zone measured in cell diameters displayed a similar age-related decline (**Fig.7H**). Thus, the extent of LST-1 expression displayed age-related decline by day 3, indicating there is an age-related decline in the GLP-1/Notch signaling system that maintains germline stem cells.

Development • Accepted manuscript

## Discussion:

**Sporadic changes contributed to age-related reproductive decline in a subset of animals, but population-wide changes accounted for reproductive aging in the majority of animals.**

An important issue in understanding the biology of aging is distinguishing the roles of "stochastic" versus "deterministic" changes. Experimental data can be used to categorize changes as low-frequency (sporadic) versus high-frequency (pervasive, population-wide). The next layer of interpretation suggests that low-frequency or sporadic changes have a mechanism that is stochastic, probabilistic, or unpredictable. In aging studies, the cause of such changes is inferred to be entropy, an energetic environment that damages biological systems in unpredictable ways that cause degeneration. By contrast, high-frequency or population-wide changes are inferred to have a mechanism that is programmed, deterministic, or predictable, which arises from genetic programs, such as those that control development.

Here we documented both low-frequency, sporadic changes as well as high-frequency, population-wide changes. Some defects occurred so infrequently that we could not quantify them, whereas the appearance of endomitotic oocytes in the proximal germline and a shifted DTC nucleus could be quantified; by day 5, ~9% and ~17% of germlines displayed endomitotic oocytes and a shifted DTC nucleus, respectively. There was no correlation between the appearance of these two defects in individual animals, indicating that they do not share a common cause. A longitudinal study indicated that the presence of endomitotic oocytes reduced progeny production, consistent with previous studies of mutant strains that display high levels of endomitotic oocytes and are subfertile or sterile (Greenstein, 2005; Iwasaki et al., 1996; McCarter et al., 1997; Wormbase WS260, 2017). These results suggest that low-frequency, sporadic defects account for age-related decrease in progeny production in a subset of animals (**Fig.8C**). Similar to these results, sporadic defects of mispositioned niche cells and ectopic germ cell proliferation were reported in a subset of middle-aged *Drosophila* ovaries (Kao et al., 2015).

A variety of high-frequency, population-wide changes were observed by analyzing the stem cell pool and mitotic cell cycle. Striking declines in germline function were observed very early in life, at day 3 of adulthood when each animal was still producing >100 progeny per day, including a 25% decrease in PZ cell number, a 1.4-fold decrease in stem cell number, a doubling of the cell cycle duration, and a 5-fold decrease in the rate of meiotic entry. Due to the assembly-line organization of the germline, these declines in distal germline function were manifested at day 5, contributing at least in part to the 4-fold decrease in progeny production (**Fig.8A,B**). Further distal germline declines on day 5 were manifested as decreased progeny production on day 7 and beyond. These age-related changes appeared to occur in all animals, and thus were quite different from the low-frequency changes. These studies suggest that population-wide changes are the predominant cause of the age-related decline in progeny production (**Fig 8C**). Furthermore, we found a significant correlation between gonad arms in the decrease in PZ size, indicating that there is an age-related systemic change, likely cell non-autonomous, that results in a functional decline in both germlines.

Previous studies of *C. elegans* aging in the distal germline focused on sperm-depleted and/or older animals. The progenitor zone shrinks with age, and mating enhances this phenotype through promoting germ cell flux; TGF-β and insulin signaling pathways accelerate

Development • Accepted manuscript

these changes (Luo et al., 2010; Narbonne et al., 2015; Qin and Hubbard, 2015). By contrast, we examined sperm-replete animals prior to and during the rapid decrease in reproductive output using mated hermaphrodites. Male exposure might have multiple effects on hermaphrodites, including male pheromones, seminal fluid, and physical trauma (Maures et al., 2014; Shi and Murphy, 2014), and we cannot formally separate these possible effects from sperm transfer. However, self-fertile and mated day 3 hermaphrodites displayed no difference in the size of the progenitor zone, suggesting that the age-related decline in progenitor zone size was not caused by male exposure.

**Age-related changes in Notch signaling and mitotic cell cycling were associated with reproductive decline**

GLP-1/Notch signaling is necessary for the germline stem cell fate (Austin and Kimble, 1987). Based on our observation that the size of the PZ declined with age, we hypothesized that the extent of GLP-1/Notch signaling declines with age, leading to a decrease in germline stem cell number. We measured the extent of expression of two GLP-1/Notch effectors, *sygl-1* and *lst-1*; these genes are direct transcriptional targets of the GLP-1/Notch intracellular domain transcription complex and are redundantly necessary and singly sufficient for the stem cell fate (Kershner et al., 2014; Lee et al., 2016). Expression of SYGL-1 encompassed ~81 distal-most cells in day 1 adults, decreasing by ~1.4-fold at day 3. As SYGL-1 expression is sufficient for the stem cell fate, the number of SYGL-1 expressing cells provides a measure of stem cell number (Shin et al., 2017). LST-1 expression was more limited, in the 38 distal-most cells in day 1 adults, decreasing ~1.4-fold at day 3. Interestingly, single molecule fluorescent *in situ* hybridization showed that the transcription of introns for both *lst-1* and *sygl-1* extends only ~5 cell diameters from the DTC (Lee et al., 2016), which closely matches the region of LST-1 accumulation, but is significantly shorter than that of SYGL-1 accumulation, consistent with posttranscriptional mechanisms functioning in extending SYGL-1 expression (Shin et al., 2017). We suggest that LST-1 is a more direct readout of the amount of GLP-1/Notch signaling and thus propose that GLP-1/Notch signaling decreases in day 3 and 5 adults. This proposal is consistent with the age-dependent enhancement of the premature meiotic entry phenotype in a weak *glp-1* loss-of-function mutant (Qin and Hubbard, 2015). One way to test the hypothesis that the age-related decline in Notch signaling is a cause of reproductive aging is to analyze mutant strains with altered Notch signaling. Chromosomal mutations that increase *glp-1* activity and transgenic constructs that increase *sygl-1* activity have been reported (Pepper et al., 2003; Shin et al., 2017), and if these manipulations delay reproductive aging it would provide direct support for our hypothesis.

The mitotic cell cycle duration doubled by day 3 of adulthood, with the proportions of the cell cycle phases unchanged and no cell cycle quiescence. Similarly, there is a slowing of cell cycle duration in *Drosophila* female germline aging (Kao et al., 2015). The doubling of cell cycle duration is not due to a decrease in GLP-1/Notch signaling, as cell cycle duration is unaffected in weak *glp-1* loss-of-function mutants that decrease stem cell number (Lee et al., 2016; Fox and Schedl, 2015). In contrast to aging in day 3 mated adults, starvation at various life cycle stages (L1, L2 and mid-L4) results in germline quiecence, with a G2 cell cycle arrest (Baugh, 2013; Fukuyama et al., 2006; Narbonne et al., 2015; Seidel and Kimble, 2015). Likewise, PZ quiescence in the absence of sperm also appears to be in G2-phase (Narbonne et al., 2015; Qin and Hubbard, 2015). Thus, the mechanisms affecting cell cycle changes during aging in mated

Development • Accepted manuscript

hermaphrodites appear to be distinct from those described to occur during starvation and the absence of sperm. The doubling of cell cycle duration and the decrease in stem cell number (GLP-1/Notch signaling) provide an informed point to further define the systemic molecular mechanisms that account for the rapid, population-wide changes in the distal germline.

**The evolutionary biology of reproductive aging**

Detailed measurements of reproductive aging raise the intriguing question: what selective forces during evolution sculpted the progeny production curve so that it displays such a dramatic decline early in life? Two long-standing theories are based on the premise that an organism achieves reproductive success by generating as many progeny as possible. According to this logic reproductive aging is a deleterious trait because it decreases progeny production. Medawar (1952) proposed that extrinsic mortality creates a "shadow of selection" that gradually prevents natural selection from favoring animals with a longer reproductive span. Williams (1957) proposed that selection for high levels of early reproduction causes a decline of late reproduction as a result of antagonistically pleiotropic genes. By contrast, the optimal progeny number theory proposed by Hughes et al. (2007) is based on the premise that an organism achieves reproductive success by generating an optimal number of progeny – not too few and not too many. According to this logic, reproductive aging is an adaptive trait that contributes to sculpting the progeny production curve to achieve the optimal number. It is apparent that reproductive success is not as simple as the number of F1 progeny generated by the P0 parent – a more sophisticated perspective is the number of F1 progeny that mature to be reproductive adults and generate F2 progeny. The extension of this logic is that reproductive success must be judged based on an organism's long-term contribution to the gene pool measured after innumerable generations. Thus, reproductive success is related to long-term population dynamics. Individuals are part of populations that exist in ecological niches with finite resources. If the population exceeds the carrying capacity of the ecological niche, then there will be widespread deprivation and population instability characterized by cycles of boom and bust. Thus, reproductive success is fostered by individual reproductive patterns that promote stable population dynamics. By limiting progeny production, reproductive aging may be a cause of reproductive restraint that promotes the optimal progeny number and leads to adaptive population dynamics.

The results presented here do not directly test evolutionary theories, but they relate to these theories in two important ways. First, we demonstrated that reproductive aging in *C. elegans* is primarily caused by population-wide changes in stem cell number and activity and only rarely caused by sporadic defects such as endomitotic oocytes. This pattern is suggestive of an evolved genetic program that controls the decline of reproduction, consistent with a prediction of the optimal progeny number theory. Second, our results document a very early decline in germline function, long before comparable declines in somatic function. This pattern suggests that during evolution somatic tissues were selected to be durable during the rise and fall of reproductive function, so that somatic aging does not limit reproduction. We speculate that this pattern facilitates selection to accelerate or delay reproductive aging as a way to manipulate progeny number, since somatic function is not the limiting factor. An important test of these evolutionary theories will be to experimentally determine how reproductive aging influences population dynamics over many generations. To this end we are developing a laboratory ecosystem to measure population dynamics and a simulation model to determine how the progeny production curve and reproductive aging affect population dynamics.

Development • Accepted manuscript

## Materials and Methods

### Strains and General Methods

*C. elegans* strains were cultured at 20°C on 6 cm Petri dishes containing nematode growth media (NGM) agar and a lawn of *E. coli* strain OP50 unless otherwise noted. The wild-type *C. elegans* strain and parent of edited strains was Bristol N2 (Brenner, 1974). Mated, wild-type N2 hermaphrodites were used except: unmated self-fertile N2 hermaphrodite data (**Fig.1A,S5**) and mated hermaphrodites with the genotype *lst-1(am302)* and *sgyl-1(am307)* in which the endogenous loci encode the FLAG epitope (**Fig.7,S10**).

Males of the strain CB4855 ("Mr. Vigorous") were used to mate hermaphrodites because these males display a higher mating ability – they also deposit a copulatory plug after mating (Hodgkin and Doniach, 1997). Strains were obtained from the CGC unless otherwise noted.

Animals were synchronized by picking fourth-stage larvae (L4), defined as day 0, from populations that had not experienced starvation for a minimum of three generations. For mating experiments, 30-50 L4 hermaphrodites were cultured on a dish with 30-50 young adult males (at a 1:1 ratio) for 24 hours, then the hermaphrodites were removed from the males. The presence of copulatory plugs on many of the hermaphrodites confirmed a high frequency of mating in the population; however, hermaphrodites without a copulatory plug were not excluded from the experiment. Hermaphrodites were moved to fresh NGM+*E. coli* OP50 dishes daily until they reached the desired age.

To measure progeny production of mated hermaphrodites, we placed 30 L4, wild-type hermaphrodites and 30 young adult, CB4855 males on a Petri dish with abundant food for 24 hours. After 24 hours (adult day 1), we placed each mated hermaphrodite on an individual dish, transferred the animal to a fresh dish daily, and two days later scored the number of live progeny produced daily. This method provides accurate and precise measurements of daily progeny production, consistent with previous findings (Hughes et al., 2007). Because animals were mated in groups, we did not obtain progeny counts for the first 24 hours for the mated animals in **Fig.1A**. To measure progeny production of self-fertile hermaphrodites, we placed each L4 hermaphrodite on an individual dish, transferred the animal to a fresh dish daily, and two days later scored the number of live progeny on the dish.

Previous studies showed that exposure to a high concentration of males or male pheromone reduced longevity and caused shrinking of hermaphrodites (Maures et al., 2014; Shi and Murphy, 2014). The damage appears to be caused by functional sperm,but not seminal fluid (Shi and Murphy, 2014). In the experiments described here, male exposure was limited to the minimum required for sperm transfer. Under these conditions, day 3 adults that were mated and self-fertile displayed a similar size of the distal germline or extent of the PZ (**Fig.S5**); at day 3 most of the unmated hermaphrodites are still self-fertile, and thus the PZ has not become quiescent due to the absence of sperm (Narbonne et al., 2015; Qin and Hubbard, 2015). Previous work in our labs showed no effect of brief mating on the longevity of hermaphrodites (Pickett et al., 2013).

Development • Accepted manuscript

**Generating alleles encoding the FLAG epitope using CRISPR/Cas9**

To visualize the localization of LST-1 and SYGL-1, we engineered alleles that encode the FLAG epitope (C-terminal *lst-1(am302[lst-1::flag])*, in which all 6 predicted LST-1 isoforms are fused to FLAG, and N-terminal *sygl-1(am307[flag::sygl-1])*. Generally, the co-CRISPR approach was used to edit genomic loci (Arribere et al., 2014). Guides and repair templates were designed in ApE (Davis, 2016) (**Table 1**). Oligonucleotides and gblocks were purchased from IDT. gblocks were amplified by PCR, purified using an Invitrogen PCR cleanup kit, concentrated using ethanol precipitation, and then resuspended in Tris-EDTA buffer. Guide oligonucleotides were ligated into Mike Nonet's derivative of pDR274 (previously digested with BsaI-HF and purified on a Quiagen column) to generate guide RNA expression plasmids, which were transformed into competent DH5-alpha cells. Plasmids were purified using a Quiagen miniprep column according to manufacturer's instructions, including the extra PB wash, and resuspended in Tris-EDTA buffer. All new plasmids were confirmed by sequencing.

Injection mixes were diluted into water and contained Cas9-expressing pDD162 (gift of Mike Nonet) at 50ng/ul, *dpy-10* guide plasmid (pMN3153) at 20ng/ul, *dpy-10(cn64)* repair oligonucleotide AFZF827 at 500nM, our gene-of-interest guide plasmids at 40ng/ul for each plasmid, a ssDNA repair template at 600nM or a dsDNA repair template at between 50ng/ul and 500ng/ul. Approximately 30 young adult P0 animals were injected in one or both gonads and recovered in recovery buffer (5mm HEPES pH 7.2, 3 mM CaCl2, 3 mM MgCl2, 66 mM NaCl, 2.4 mM KCl, 4% Glucose (w/v)) on NGM dishes.

Young adult F1 hermaphrodites were screened for the Rol or Dpy phenotype, and mutant animals were picked singly or in groups of up to 8 to fresh NGM dishes and allowed to produce progeny overnight. Next, animals were picked into 10ul of 1X PCR buffer containing 0.1 mg/mL Proteinase K, incubated at 65 °C for 60 minutes and then at 95 °C for 30 minutes to inactivate Proteinase K. Using primers that hybridize outside of the homology template, PCR was used to detect insertions of 66nt (New England Biological). The young adult F2 progeny of homozygous or heterozygous edited F1 animals were picked to individual dishes and genotyped in a similar manner. The DNA sequence of the PCR product from homozygous edited F2 progeny was determined to confirm the in-frame insertion of DNA encoding the FLAG epitope. Strains were outcrossed to N2, resulting in WU1756 and WU1770 for *lst-1* and *sygl-1*, respectively. Our working protocol is available at http://notthatkindofworm.wikia.com/wiki/Worm_CRISPR .

To address the possibility that insertion of DNA encoding the epitome tag disrupted the activity of the *lst-1* or *sygl-1* gene, we performed a functional test. Neither *lst-1(null)* nor *sygl-1(null)* single mutants display a visible phenotype, whereas *lst-1(null);sygl-1(null)* double mutants (or double RNAi knockdowns) display a sterile phenotype. We used RNAi to knock down the expression of *sygl-1* in *lst-1(am302)* animals or *lst-1* in *sygl-1(am307)* animals. We did not observe a sterile phenotype in either case, indicating that these alleles retain gene activity.

**EdU labeling experiments**

To make EdU dishes, we seeded M9 agar dishes (Stiernagle, 2006) with concentrated *E. coli* MG1693 Thy- which had been grown for 24 hours at 37C with shaking in minimal media containing 20uM 5-ethynyl-2'-deoxyuridine (EdU, Invitrogen). The culture consisted of 100mL

Development • Accepted manuscript

M9, 4ml overnight LB-grown MG1693 *E. coli*, 5ml 20% glucose, 50ul 1.25mg/ml thiamine, 1.2ml 0.5mM thymidine, 100ul 1M MgSO4, 200ul 10mM EdU (Fox et al., 2011).

Appropriately mated and aged animals were either washed with phosphate buffered saline (PBS) or picked to EdU dishes and incubated for the appropriate time: 0.5, 4, 7, or 10 hours. Cells with any amount of EdU signal overlapping with DAPI staining were scored as EdU-positive. We defined S-phase index as the proportion of all progenitor zone cells (WAPL-1-positive) that were also EdU-positive. For the full detailed protocol, see Kocsisova et al. (2018a)

In day 5 hermaphrodites, a subpopulation displayed robust EdU labeling and a subpopulation displayed a complete lack of EdU labeling (**Fig.S6A-C**). When fed EdU for 0.5 hours, 85% of day 5 animals showed no EdU-positive cells. In the remaining 15% of animals, the average S-phase index was 53% (range 31.5 - 76.7% of cells), which is not significantly different than the S-phase index for day 1 or 3 hermaphrodites (**Fig.4G**). In 29 of 33 day 5 animals fed EdU for 0.5 hours where both germlines were visible, either both germlines displayed EdU incorporation or both germlines displayed no EdU incorporation (intraclass correlation coefficient = 0.75, $p<0.0001$). In the remaining 4 of 33 day 5 animals, two germlines were discordant for EdU labeling (**Fig.S6D**). Soaking day 5 animals in a solution of 500 μM EdU in M9, as described in Furuta et al., (2018), also resulted in a subpopulation that completely lacked EdU labeling. As the duration of EdU feeding increased, so did the proportion of animals showing labeling. When day 5 animals were fed EdU for 4 hours, 81% of animals displayed EdU-positive cells (range 48.1% to 94.4% of cells). Our observation that older animals frequently displayed no EdU incorporation following a short duration of EdU exposure but only infrequently displayed this following a longer duration of EdU exposure is similar to findings reported by Cinquin et al., (2016).

We observed that both EdU-positive and EdU-negative animals displayed EdU labeled bacteria in the intestinal lumen, indicating that both groups of animals successfully ingested EdU labeled bacteria. One possible explanation for animals that do not incorporate EdU is that some day 5 hermaphrodites are inefficient in intestinal absorption of EdU, transport of EdU to the germline, and/or incorporation of EdU into DNA. Alternatively, some day 5 hermaphrodites may be susceptible to trauma following transfer from one dish to another, resulting in a temporary block in EdU incorporation. Alternatively, in some day 5 hermaphrodites all progenitor zone cells may be arrested in a cell cycle phase other than S-phase. In this case, the arrest appears to be transient, because we observed (a) scattered M-phase cells in germlines that lacked EdU labeling, indicating that in these germlines most cells were in a Gap-phase or arrested while others were in M-phase, (b) longer durations of EdU exposure resulted in a significantly higher proportion of EdU labeled animals, and (c) in EdU pulse-chase experiments, the distal germline did not contain cells with intense EdU labeling, indicating that all stem cells underwent several cell divisions during the 48 hour chase. To our knowledge, there is no method to unambiguously identify S-phase cells in the *C. elegans* germline without feeding or injecting nucleotide analogs (Kocsisova et al., 2018a; Kocsisova et al., 2018b; van den Heuvel and Kipreos, 2012).

Development • Accepted manuscript

## Dissection and Immunohistochemistry

The dissection and staining protocol follows the batch method (Francis et al., 1995), where all dissected tissues were incubated within small glass tubes rather than on a slide. Animals were washed with phosphate-buffered saline (PBS) into a dissecting watchglass (Carolina Biological Item # 742300), immobilized with Levamisole (final concentration 200uM), and dissected with a pair of 25G 5/8" needles (PrecisionGlide from BD) by cutting at the pharynx and/or at the tail. Dissected gonads were fixed in 2 mL 3% paraformaldehyde (PFA) (10 mL 16% PFA, EM Grade, Electron Microscopy Sciences, Hatfield, PA Catalog No 15710) phosphate-buffered solution for 10 minutes at room temperature and then post-fixed with 2 mL 100% methanol (Gold-label from Fisher) at -20C for 1 hour or longer (up to several days).

In the past there were discrepancies in the literature possibly due to different analysis methods in very old worms: in situ analysis versus dissected gonads. To circumvent this issue, we performed dissections at time points when these discrepancies are less likely to be a problem.

Fixed gonads were rehydrated and washed three times in PBS + 0.1% Tween-20 (PBSTw), then incubated in 100ul of primary antibody at room temperature for 4-24 hours, washed 3 times in PBSTw, and incubated in 100ul of secondary antibody at room temperature or 4C for 2-24 hours. Antibodies were diluted in 30% goat serum (Gibco C16210-072) in PBS. Primary antibodies used were: rabbit-anti-WAPL-1 (Novus Biologicals Cat#49300002, Lot G3048-179A02) (1:2000), mouse-anti-MSP (Major Sperm Protein) (Miller et al., 2001) (1:2000), mouse-anti-pH3 (Millipore clone 3H10 Cat#05-806, Lot#2680533) (1:500), mouse-anti-FLAG (SIGMA M2, purified in-house) (1:1000). Secondary antibodies were: goat-anti-mouse IgG-conjugated Alexa Fluor 488/594/647, goat-anti-rabbit IgG-conjugated Alexa Fluor 488/594/647 (Invitrogen).

Following antibody staining, gonads were washed 3 times in PBSTw. An EdU Click-iT reaction was performed according to manufacturer's instructions (Invitrogen C10350), using 100ul reagent for a 30 minute incubation, followed by a quick wash in manufacturer-supplied rinse buffer and four ~15 minute washes in PBSTw. Stained gonads were resuspended in 1 drop of Vectashield containing 4',6-Diamidino-2-Phenylindole Dihydrochloride (DAPI) (Vector Laboratories H-1200), applied to a large pre-made agarose pad on a glass slide, and covered with a 22 mm x 40 mm #1 cover glass. The slide was allowed to settle overnight at room temperature, sealed with clear nail polish, and stored at 4 °C as needed. Images were acquired within 72 hours when possible.

## Confocal Imaging

Images were collected using a Zeiss Plan Apo 63X 1.4 oil-immersion objective lens on a PerkinElmer Ultraview Vox spinning disc confocal system on a Zeiss Observer Z1 microscope using Volocity software. Approximately twenty 1 μm z-slice images were acquired for each gonad. Images were exported as hyperstack .tif files for further analysis.

## Image analysis

Images were stitched either in Volocity or using the Image J plugins for pairwise stitching and Grid/Collection of sequential images (Preibisch et al., 2009). Images were rotated, cropped, arranged, and annotated in Illustrator (Adobe).

Development • Accepted manuscript

Cells were manually counted in each z-slice where they occurred. The person performing counts was not blinded to experimental groups, because the differences were generally obvious to an experienced observer. Counts of cells were performed in Fiji/ImageJ (Schindelin et al., 2012) using the Cell Counter plug-in (De Vos, 2015; Rasband, 2016). To remove multiply-counted cells, a modified version of the R-script Marks-to-Cells was used (Seidel and Kimble, 2015). This script improved the precision of cell counts in the germline.

Nuclear morphology: DAPI staining was used to assess meiotic prophase stages, nuclear counts, row counts and progression of gametogenesis. Endomitotic oocytes in the proximal gonad arm, distal to the spermatheca, were recognized as large DAPI stained blobs. Endomitotic oocytes are known to result from failure to coordinate meiotic maturation of diakinesis stage oocytes with ovulation, resulting in the unfertilized mature oocytes that are mitotic cell cycling without cytokinesis because of the absence of the sperm derived centriole (Greenstein, 2005; Iwasaki et al., 1996; McCarter et al., 1997). This is distinct from endomitotic oocytes in the uterus, which naturally occur in older unmated hermaphrodites that have exhausted their self-sperm. In this case the most proximal oocyte undergoes low-frequency spontaneous maturation and ovulation, but because there is no sperm in the spermatheca the matured but unfertilized oocyte begins endomitotic cycling (McCarter et al., 1999). Endomitotic oocytes were identified from dissected germlines; as the proximal germline was not always visible, this raises the possibility that the frequency was under-estimated.

Distal tip cell nucleus: The DTC nucleus was identified by its position at the exterior of the distal gonad and bright WAPL-1 staining. When analyzing the shift of the DTC nucleus, we chose a stringent cutoff of 5 c.d., because of a concern that a DTC nucleus might shift by one or two c.d. due to physical forces during dissection and staining. We did analyze our data with the cutoff set to 2 c.d., and even with this broad definition of "shifted" DTC nucleus, the majority of germlines were "normal".

Progenitor zone: The PZ has been previously called the mitotic zone or the proliferative zone. We employed staining with the cohesin chaperone WAPL-1 to measure the size of the PZ (Mohammad et al., 2018). In mated hermaphrodites, the total number of PZ cells was 215 +/- 25 in day 1 adults, and it decreased to 163 +/- 47 in day 3 animals, and to 126 +/- 45 in day 5 animals. A similar number of PZ cells, ~230, was found for day 1 unmated hermaphrodites using a combination of the nucleoplasmic REC-8 staining PZ marker and the meiotic prophase marker HIM-3 (Fox and Schedl, 2015; Fox et al., 2011; Hansen et al., 2004). Other studies of unmated day 1 hermaphrodites used the crescent-shaped DAPI morphology of leptotene cells to approximate the proximal boundary of the PZ and found that the PZ contains ~214 (Korta et al., 2012), ~205 (Roy et al., 2016) or ~225 cells (Seidel and Kimble, 2015). Our day 1 PZ cell numbers for mated hermaphrodites are thus similar to PZ cell numbers for unmated day 1 hermaphrodites reported in other studies; therefore, mating did not have a significant effect on PZ cell numbers at day 1. Prior studies of changes in PZ cell number during aging with unmated hermaphrodites report the following: Hubbard and colleagues found ~250 PZ cells in day 1 adults, ~156 by day 3, ~100 by day 6, ~50 by day 12 (Killian and Hubbard, 2005; Qin and Hubbard, 2015); Murphy and colleagues reported a decrease in PZ cell number from ~220 at day 2 to ~150 at day 6 in unmated hermaphrodites (Luo et al., 2010); and Kimble and colleagues reported that PZ cell number remained unchanged up to day 6 of adulthood (day 1 ~243, day 2 ~227, day 3 ~214) (Crittenden et al., 2006). In mated hermaphrodites, Shi and Murphy (2014) found a decrease in the number of PZ cells with age, from ~150 in day 1 to ~100 in day 2

Development • Accepted manuscript

through day 4. However, under the conditions employed the mated hermaphrodites displayed damage to the soma (body size shrinkage), which was not the case with the conditions employed in the experiments described here. The Hubbard and Narbonne groups reported that starting at day 3 and older, when unmated hermaphrodites have become sperm depleted (or in younger adult genetic females), the absence of sperm, and thus flux through the germline, results in mitotic cell cycle arrest of PZ cells, likely in G2 phase (Narbonne et al., 2015; Qin and Hubbard, 2015). One interpretation of this finding is that the mitotic cell cycle quiescence of the PZ in the absence of sperm is a physiological mechanism of preserving the germline during aging, in anticipation of subsequent mating. To avoid this preservation mechanism in our studies of germline aging, we always used mated hermaphrodites.

M-phase cells and the presence of sperm: Cells in M-phase were detected by staining with mouse anti-phospho-histone 3 (pH3) antibody, while sperm were identified by staining with mouse anti-MSP (Major Sperm Protein) antibody. In these co-staininig experiments, M-phase cells and sperm were distinguished by (1) position in the germline and (2) DAPI morphology; M-phase cells were in the PZ at the distal end of the germline, while sperm were in the spermatheca at the proximal end of the gonad. Stages of M-phase (prophase, metaphase & anaphase) were analyzed in cells detected with pH3 antibody; minimal differences were observed between day 1, 3 and 5 (**Fig.S7**).

SYGL-1 and LST-1: The length in cell diameters and the number of cells in the PZ that contain cytoplasmic SYGL-1 and LST-1 were assessed with anti-FLAG antibody staining using strains in which CRISPR genome editing was employed to insert DNA encoding a 3xFLAG epitope into the endogenous locus. In day 1 animals, we observed staining similar to that reported by Shin et al. (2017). However, we note that at day 3 and 5, the length of the SYGL-1 staining region could be similar to the length of the PZ, as assessed by WAPL-1 staining (i.e. only a few WAPL-1-positive, SYGL-1 negative cells were observed).

Germline stem cell differentiation occurs through essentially direct differentiation and thus lacks transit-amplifying divisions; following loss of GLP-1 Notch signaling, germ cells complete their ongoing mitotic cell cycle and then begin meiotic S-phase (Fox and Schedl, 2015). SYGL-1 activity is sufficient for the stem cell fate (Kershner et al., 2014; Lee et al., 2016; Shin et al., 2017). However, it is unknown if all cells that are expressing endogenous levels of SYGL-1 are stem cells. There is a noticeable gradient of SYGL-1 staining between the highly-expressing distal-most and lowly-expressing proximal-most cells, raising the possibility that the level of SYGL-1 in the proximal-most cells is not sufficient to promote the stem cell fate and inhibit the meiotic fate. Additionally, Spike et al. (2018) have shown that RNA binding proteins LIN-41 and GLD-1 are post-translationally inactivated prior to their degradation; similarly, proximal SYGL-1 may be inactivated prior to degradation. Thus, while the extent of SYGL-1 accumulation provides a readout that is correlated with stem cell identity, detectable SYGL-1 accumulation cannot currently be used to define the number of stem cells.

Meiotic entry and nurse cells: Most cells that exit the progenitor zone and enter meiosis in an adult hermaphrodite do not become oocytes. Instead, these cells function as nurse cells and undergo apoptosis. We calculated the nurse cell proportion following the method outlined in Agarwal et al. (2018). We compared the output of the progenitor zone on days 1, 3, and 5 (**Fig.5B, Supplemental Table 5**) to the number of embryos (and therefore oocytes) produced on days 3, 5, and 7, then divided by 2 to account for two gonads per animal (**Fig.1A, Supplemental Table 1**). The two-day difference was used to account for the time required for a

Development • Accepted manuscript

cell to progress through meiotic prophase (**Fig.S9, Supplemental Table S8**). We defined the nurse cell proportion as 1-( 0.5 * # oocytes per hour / # cells entered meiosis per hour in one gonad).

**Statistical Analysis**

Statistical analyses were performed in R (R Core Team, 2013) using R studio (RStudio Team, 2015) and the following packages: ggplot2 (Wickham, 2009), svglite, plyr, gridExtra, grid, lattice, multcomp, car, broom, psych, FSA, fifer. Individual measurements and script used to analyze them are provided in Supplemental Tables and files. Depending on the type of variable, the following tests were performed and are indicated in the text and Figure legends with the relevant test name abbreviation. KW test: for continuous measurement variables, the Kruskal-Wallis Rank-sum test was used with a Dunn post-hoc and p-values adjusted with the Benjamini-Hochberg FDR method. Data were also compared using an ANOVA with a Tukey post-hoc test. PC test: for categorical measurement variables, the Pearson's Chi-squared test of independence was used with post-hoc p-values adjusted with the False Discovery Rate method. PIC test: to test for linear relationships between variables, we used the Pearson's *inter*class correlation. ICC test: used for *intra*class correlations to compare the pooled variance between pairs of germlines from one animal and pooled variance within pairs (Shrout and Fleiss, 1979). Boolean variables were treated as TRUE = 1, FALSE = 0 for purposes of correlation analysis. All error bars shown in figures represent the mean +/- standard deviation. NS indicates $P>0.05$, * $P<0.05$, ** $P<.001$, *** $P<.0001$.

All data were subjected to consistent exclusion criteria. Animals that displayed evidence of matricidal hatching or sperm depletion (as indicated by lack of Major Sperm Protein immunofluorescence) were excluded from all analyses. Animals that displayed sporadic phenotypes such as endomitotic oocytes, a shifted DTC nucleus, or failure to exhibit any EdU staining are reported, but were excluded from further analyses. Exact statistical methods and exclusion criteria are provided in the supplemental R script.

Development • Accepted manuscript

## Acknowledgements:

We are grateful to the *E. coli* stock center for MG1693; Wormbase; the *Caenorhabditis* Genetics Center which is funded by the National Institutes of Health Office of Research Infrastructure Programs (P40OD010440) for strains; Mike Nonet and Scott Dour for advice, reagents, and injection microscope use for CRISPR/Cas9 genome engineering; Zach Pincus for statistical advice and injection microscope use; Aiping Feng for reagents; Luke Schneider, Andrea Scharf, Sandeep Kumar, Ariz Mohammad, and John Brenner for training, advice, support, reagents, and helpful discussion; and the Kornfeld and Schedl labs for feedback on this manuscript. Finally, we are grateful to three anonymous reviewers for suggestions that greatly improved the manuscript.

**Competing interests:** No competing interests declared.

**Funding:** This work was supported in part by the National Institutes of Health [R01 AG02656106A1 to KK, R01 GM100756 to TS], a National Science Foundation predoctoral fellowship [DGE-1143954 and DGE-1745038 to ZK], and The Douglas Covey Fellowship to ZK. Neither the National Institutes of Health, the National Science Foundation, nor Douglas Covey had any role in the design of the study, collection, analysis, and interpretation of data, nor in writing the manuscript.

**Authors' contributions:** ZK, KK, and TS designed the study. ZK performed experiments, analyzed data, and wrote the manuscript. ZK, KK, and TS revised the manuscript. All authors read and approved the final manuscript.

**Abbreviations Used**:

Phosphate Buffered Saline (PBS)
4',6-Diamidino-2-Phenylindole, Dihydrochloride (DAPI)
5-ethynyl-2'-deoxyuridine (EdU)
Distal Tip Cell (DTC)
Progenitor Zone (PZ)
Endomitotic Phenotype (Emo)
untranslated region (UTR)
cell diameters (c.d.)

Development • Accepted manuscript

## Literature Cited


**Agarwal, I., Farnow, C., Jiang, J., Kim, K. S., Leet, D. E., Solomon, R. Z., Hale, V. A. and Goutte, C.** (2018). HOP-1 presenilin deficiency causes a late-onset notch signaling phenotype that affects adult germline function in caenorhabditis elegans. *Genetics* **208**, 745–762.

**Angeles-Albores, D., Leighton, D. H. W., Tsou, T., Khaw, T. H., Antoshechkin, I. and Sternberg, P. W.** (2017). The Caenorhabditis elegans Female State: Decoupling the Transcriptomic Effects of Aging and Sperm-Status. *G3: Genes, Genomes, Genetics* **7**, 2969–2977.

**Angelo, G. and Van Gilst, M. R.** (2009). Starvation Protects Germline Stem Cells and Extends Reproductive Longevity in C. elegans. *Science* **326**, 954–958.

**Arribere, J. A., Bell, R. T., Fu, B. X. H., Artiles, K. L., Hartman, P. S. and Fire, A. Z.** (2014). Efficient marker-free recovery of custom genetic modifications with CRISPR/Cas9 in Caenorhabditis elegans. *Genetics* **198**, 837–846.

**Austin, J. and Kimble, J.** (1987). glp-1 is required in the germ line for regulation of the decision between mitosis and meiosis in C. elegans. *Cell* **51**, 589–599.

**Baugh, L. R.** (2013). To grow or not to grow: Nutritional control of development during Caenorhabditis elegans L1 Arrest. *Genetics* **194**, 539–555.

**Brenner, S.** (1974). The genetics of Caenorhabditis elegans. *Genetics* **77**, 71–94.

**Cinquin, A., Chiang, M., Paz, A., Hallman, S., Yuan, O., Vysniauskaite, I., Fowlkes, C. C. and Cinquin, O.** (2016). Intermittent Stem Cell Cycling Balances Self-Renewal and Senescence of the C. elegans Germ Line. *PLoS Genetics* **12**, e1005985.

**Crittenden, S. L., Leonhard, K. A., Byrd, D. T. and Kimble, J.** (2006). Cellular analyses of the mitotic region in the Caenorhabditis elegans adult germ line. *Molecular biology of the cell* **17**, 3051–61.

**Davis, M. W.** (2016). A Plasmid Editor (ApE).

**de la Guardia, Y., Gilliat, A. F., Hellberg, J. and Rennert, P.** (2016). Run-on of germline apoptosis promotes gonad senescence in C . elegans. *Oncotarget* **7**, 39082–96.

**De Vos, K.** (2015). Cell Counter Plugin. https://imagej.nih.gov/ij/plugins/cell-counter.htm.

**Fox, P. M. and Schedl, T.** (2015). Analysis of Germline Stem Cell Differentiation Following Loss of GLP-1 Notch Activity in Caenorhabditis elegans. *Genetics* **201**, 167–184.

**Fox, P. M., Vought, V. E., Hanazawa, M., Lee, M.-H. H., Maine, E. M. and Schedl, T.** (2011). Cyclin E and CDK-2 regulate proliferative cell fate and cell cycle progression in the C. elegans germline. *Development* **138**, 2223–2234.

**Francis, R., Barton, M. K., Kimble, J. and Schedl, T.** (1995). gld-1, a tumor suppressor gene required for oocyte development in Caenorhabditis elegans. *Genetics* **139**, 579–606.

**Fukuyama, M., Rougvie, A. E. and Rothman, J. H.** (2006). C. elegans DAF-18/PTEN mediates nutrient-dependent arrest of cell cycle and growth in the germline. *Current biology : CB* **16**, 773–9.

**Furuta, T., Joo, H.-J., #1, K. A. T., Chen, S.-Y., Arur, S., Trimmer, K. A., Chen, S.-Y. and Arur, S.** (2018). No Title. *Development (Cambridge, England)* **145**, dev.161042.

**Garigan, D., Hsu, A. L., Fraser, A. G., Kamath, R. S., Abringet, J. and Kenyon, C.** (2002). Genetic analysis of tissue aging in Caenorhabditis elegans: A role for heat-shock factor and bacterial proliferation. *Genetics* **161**, 1101–1112.

**Greenstein, D.** (2005). Control of oocyte meiotic maturation and fertilization. *WormBook* 1–12.

**Greenwald, I. and Kovall, R.** (2013). Notch signaling: genetics and structure. In *WormBook* (ed. The C. elegans Research Community), p. 1.10.2.

**Guarente, L. and Kenyon, C.** (2000). Genetic pathways that regulate ageing in model organisms. *Nature* **408**, 255–62.

**Hansen, D. and Schedl, T.** (2013). Stem Cell Proliferation Versus Meiotic Fate Decision in


Development • Accepted manuscript

Caenorhabditis elegans. In *Germ Cell Development in C. elegans, Advances in Experimental Medicine and Biology*, pp. 71–99.

**Hansen, D., Hubbard, E. J. A. and Schedl, T.** (2004). Multi-pathway control of the proliferation versus meiotic development decision in the Caenorhabditis elegans germline. *Developmental Biology* **268**, 342–357.

**Herndon, L. A., Schmeissner, P. J., Dudaronek, J. M., Brown, P. A., Listner, K. M., Sakano, Y., Paupard, M. C., Hall, D. H. and Driscoll, M.** (2002). Stochastic and genetic factors influence tissue-specific decline in ageing C. elegans. *Nature* **419**, 808–814.

**Hirsh, D., Oppenheim, D. and Klass, M.** (1976). Development of the reproductive system of Caenorhabditis elegans. *Developmental Biology* **49**, 200–219.

**Hodgkin, J. and Doniach, T.** (1997). Natural variation and copulatory plug formation in Caenorhabditis elegans. *Genetics* **146**, 149–164.

**Hughes, S. E., Evason, K., Xiong, C. and Kornfeld, K.** (2007). Genetic and pharmacological factors that influence reproductive aging in nematodes. *PLoS Genet* **3**, e25.

**Hughes, S. E., Huang, C. and Kornfeld, K.** (2011). Identification of mutations that delay somatic or reproductive aging of Caenorhabditis elegans. *Genetics* **189**, 341–356.

**Iwasaki, K., McCarter, J., Francis, R. and Schedl, T.** (1996). emo-1, a Caenorhabditis elegans Sec61p gamma homologue, is required for oocyte development and ovulation. *J Cell Biol* **134**, 699–714.

**Jaramillo-Lambert, A., Ellefson, M., Villeneuve, A. M. and Engebrecht, J.** (2007). Differential timing of S phases, X chromosome replication, and meiotic prophase in the C. elegans germ line. *Developmental Biology* **308**, 206–221.

**Kao, S.-H. H., Tseng, C.-Y. Y., Wan, C.-L. L., Su, Y.-H. H., Hsieh, C.-C. C., Pi, H. and Hsu, H.-J. J.** (2015). Aging and insulin signaling differentially control normal and tumorous germline stem cells. *Aging Cell* **14**, 25–34.

**Kershner, A. M., Shin, H., Hansen, T. J. and Kimble, J.** (2014). Discovery of two GLP-1/Notch target genes that account for the role of GLP-1/Notch signaling in stem cell maintenance. *Proceedings of the National Academy of Sciences of the United States of America* **111**, 3739–44.

**Killian, D. J. and Hubbard, E. J. A.** (2005). Caenorhabditis elegans germline patterning requires coordinated development of the somatic gonadal sheath and the germ line. *Developmental Biology* **279**, 322–335.

**Kimble, J. and Seidel, H. S.** (2013). C . elegans germline stem cells and their niche. In *StemBook*, pp. 1–12. Harvard Stem Cell Institute.

**Kimble, J. and Ward, S.** (1988). Germ-line Development and Fertilization. *Cold Spring Harbor Monograph Archive* **17**, 191–213.

**Kocsisova, Z., Mohammad, A., Kornfeld, K. and Schedl, T.** (2018a). Cell Cycle Analysis in the C. Elegans Germline with the Thymidine Analog EdU. *Journal of visualized experiments : JoVE*. **140**, e58339–e58339.

**Kocsisova, Z., Kornfeld, K. and Schedl, T.** (2018b). Cell cycle accumulation of the proliferating cell nuclear antigen PCN-1 transitions from continuous in the adult germline to intermittent in the early embryo of C. elegans. *BMC Developmental Biology* **18**, 1–12.

**Korta, D. Z., Tuck, S. and Hubbard, E. J. A.** (2012). S6K links cell fate, cell cycle and nutrient response in C. elegans germline stem/progenitor cells. *Journal of Cell Science* **125**, 859–870.

**Lee, C., Sorensen, E. B., Lynch, T. R., Kimble, J., Parrish, S., Timmons, L., Plasterk, R., Fire, A., Singh, A., Raj, A., et al.** (2016). *C. elegans* GLP-1/Notch activates transcription in a probability gradient across the germline stem cell pool. *eLife* **5**, 269–282.

**Luo, S. and Murphy, C. T.** (2011). Caenorhabditis elegans reproductive aging: Regulation and underlying mechanisms. *Genesis* **49**, 53–65.

**Luo, S., Kleemann, G. A., Ashraf, J. M., Shaw, W. M. and Murphy, C. T.** (2010). TGF-beta

Development • Accepted manuscript

and insulin signaling regulate reproductive aging via oocyte and germline quality maintenance. *Cell* **143**, 299–312.

**Maures, T. J., Booth, L. N., Benayoun, B. A., Izrayelit, Y., Schroeder, F. C. and Brunet, A.** (2014). Males shorten the life span of C. elegans hermaphrodites via secreted compounds. *Science* **343**, 541–544.

**McCarter, J., Bartlett, B., Dang, T. and Schedl, T.** (1997). Soma-germ cell interactions in Caenorhabditis elegans: multiple events of hermaphrodite germline development require the somatic sheath and spermathecal lineages. *Dev Biol* **181**, 121–143.

**McCarter, J., Bartlett, B., Dang, T. and Schedl, T.** (1999). On the Control of Oocyte Meiotic Maturation and Ovulation in Caenorhabditis elegans. *Developmental Biology* **205**, 111–128.

**Medawar, P. B.** (1952). *An unsolved problem of biology*. London: Lewis.

**Miller, M. A., Nguyen, V. Q., Lee, M. H., Kosinski, M., Schedl, T., Caprioli, R. M. and Greenstein, D.** (2001). A sperm cytoskeletal protein that signals oocyte meiotic maturation and ovulation. *Science (New York, N.Y.)* **291**, 2144–2147.

**Mohammad, A., Vanden Broek, K., Wang, C., Daryabeigi, A., Jantsch, V., Hansen, D. and Schedl, T.** (2018). Initiation of Meiotic Development Is Controlled by Three Post-transcriptional Pathways in Caenorhabditis elegans. *Genetics* **209**, 1197–1224.

**Narbonne, P., Maddox, P. S. and Labbe, J.-C.** (2015). daf-18/PTEN locally antagonizes insulin signalling to couple germline stem cell proliferation to oocyte needs in C. elegans. *Development* 4230–4241.

**Pazdernik, N. and Schedl, T.** (2013). Introduction to Germ Cell Development in Caenorhabditis elegans. In *Germ Cell Development in C. elegans, Advances in Experimental Medicine and Biology*, pp. 1–16.

**Pepper, A. S. R. S.-R., Killian, D. J. and Hubbard, E. J. A.** (2003). Genetic Analysis of Caenorhabditis elegans glp-1 Mutants Suggests Receptor Interaction or Competition. *Genetics* **163**, 115–132.

**Pickett, C. L., Dietrich, N., Chen, J., Xiong, C. and Kornfeld, K.** (2013). Mated progeny production is a biomarker of aging in Caenorhabditis elegans. *G3 (Bethesda)* **3**, 2219–2232.

**Preibisch, S., Saalfeld, S. and Tomancak, P.** (2009). Globally optimal stitching of tiled 3D microscopic image acquisitions. *Bioinformatics (Oxford, England)* **25**, 1463–5.

**Qin, Z. and Hubbard, E. J. A.** (2015). Non-autonomous DAF-16/FOXO activity antagonizes age-related loss of C. elegans germline stem/progenitor cells. *Nature communications* **6**, 7107.

**R Core Team** (2013). R: A Language and Environment for Statistical Computing. http://www.r-project.org/.

**Rasband, W. .** (2016). ImageJ. http://imagej.nih.gov/ij/.

**Roy, D., Michaelson, D., Hochman, T., Santella, A., Bao, Z., Goldberg, J. D. and Hubbard, E. J. A.** (2016). Cell cycle features of C. elegans germline stem/progenitor cells vary temporally and spatially. *Developmental Biology* **409**, 261–271.

**RStudio Team** (2015). RStudio: Integrated Development Environment for R. www.rstudio.com/.

**Schindelin, J., Arganda-Carreras, I., Frise, E., Kaynig, V., Longair, M., Pietzsch, T., Preibisch, S., Rueden, C., Saalfeld, S., Schmid, B., et al.** (2012). Fiji: an open-source platform for biological-image analysis. *Nature Methods* **9**, 676–682.

**Seidel, H. S. and Kimble, J.** (2015). Cell-cycle quiescence maintains Caenorhabditis elegans germline stem cells independent of GLP-1/Notch. *eLife* **4**, e10832.

**Shi, C. and Murphy, C. T.** (2014). Mating induces shrinking and death in Caenorhabditis mothers. *Science (New York, N.Y.)* **343**, 536–40.

**Shin, H., Haupt, K. A., Kershner, A. M., Kroll-Conner, P., Wickens, M. and Kimble, J.** (2017). SYGL-1 and LST-1 link niche signaling to PUF RNA repression for stem cell maintenance in Caenorhabditis elegans. *PLOS Genetics* **13**, e1007121.

**Shrout, P. E. and Fleiss, J. L.** (1979). Intraclass Correlations: Uses in Assessing Rater

Development • Accepted manuscript

Reliability. *Psychological Bulletin* **86**, 420–428.
**Spike, C. A., Huelgas-Morales, G., Tsukamoto, T. and Greenstein, D.** (2018). Multiple Mechanisms Inactivate the LIN-41 RNA-Binding Protein To Ensure a Robust Oocyte-to-Embryo Transition in Caenorhabditis elegans. *Genetics* **210**, 1011–1037.
**Stiernagle, T.** (2006). Maintenance of C. elegans. *WormBook* 1–11.
**van den Heuvel, S. and Kipreos, E. T.** (2012). C. elegans Cell Cycle Analysis. *Methods in Cell Biology* **107**, 265–294.
**Ward, S. and Carrel, J. S.** (1979). Fertilization and Sperm Competition in the Nematode Caenorhabditis elegans. *Developmental Biology* **73**, 304–321.
**Wickham, H.** (2009). *ggplot2: Elegant Graphics for Data Analysis*. New York: Springer-Verlag.
**Williams, G. C.** (1957). Plieotropy, natural selection, and the evolution of senescence. *Evolution* **11**, 398–411.
**Wormbase WS260** (2017).

Development • Accepted manuscript

## Figures

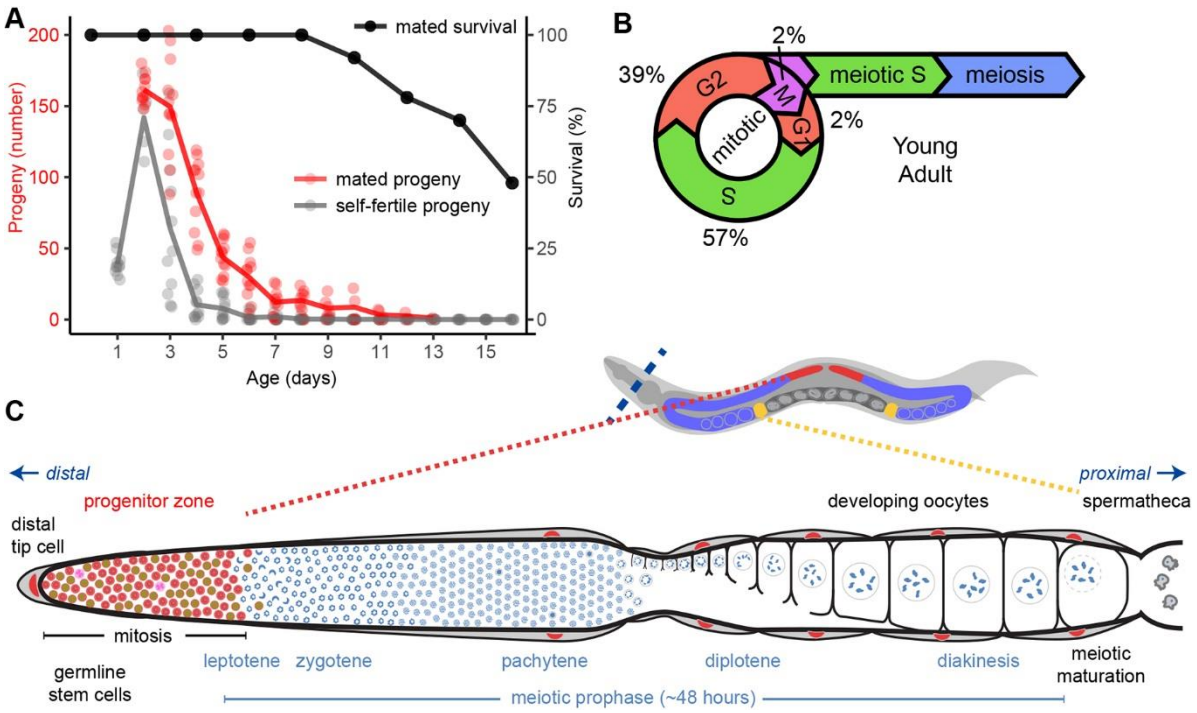


**Fig. 1: The female reproductive system displayed rapid age-related decline in sperm-replete *C. elegans***

**A)** Number of progeny produced in 24 hour intervals by a wild-type self-fertile (gray) and mated (red) hermaphrodite (n=11, 12). Day 0 defined as L4 stage. Black points indicate the percent survival of wild-type mated hermaphrodites (n=54), reproduced with permission from Pickett *et al.* (2013). (See Supplemental Table 1 for statistics)

**B)** Diagram of young adult germ cell mitotic cell cycle and meiotic entry. Numbers represent proportion of the cell cycle spent in each phase (Fox *et al.* (2011).

**C)** Diagram shows one of two gonad arms of the young adult hermaphrodite. Cells progress from mitotic cycling to meiotic prophase to meiotic maturation before being fertilized by sperm in the spermatheca (yellow). The progenitor zone (red, defined by WAPL-1 staining) contains mitotically cycling stem cells. The DTC (nucleus in red, as are other somatic gonad cells) provides GLP-1/Notch signal to maintain the germline stem cell fate.

Development • Accepted manuscript

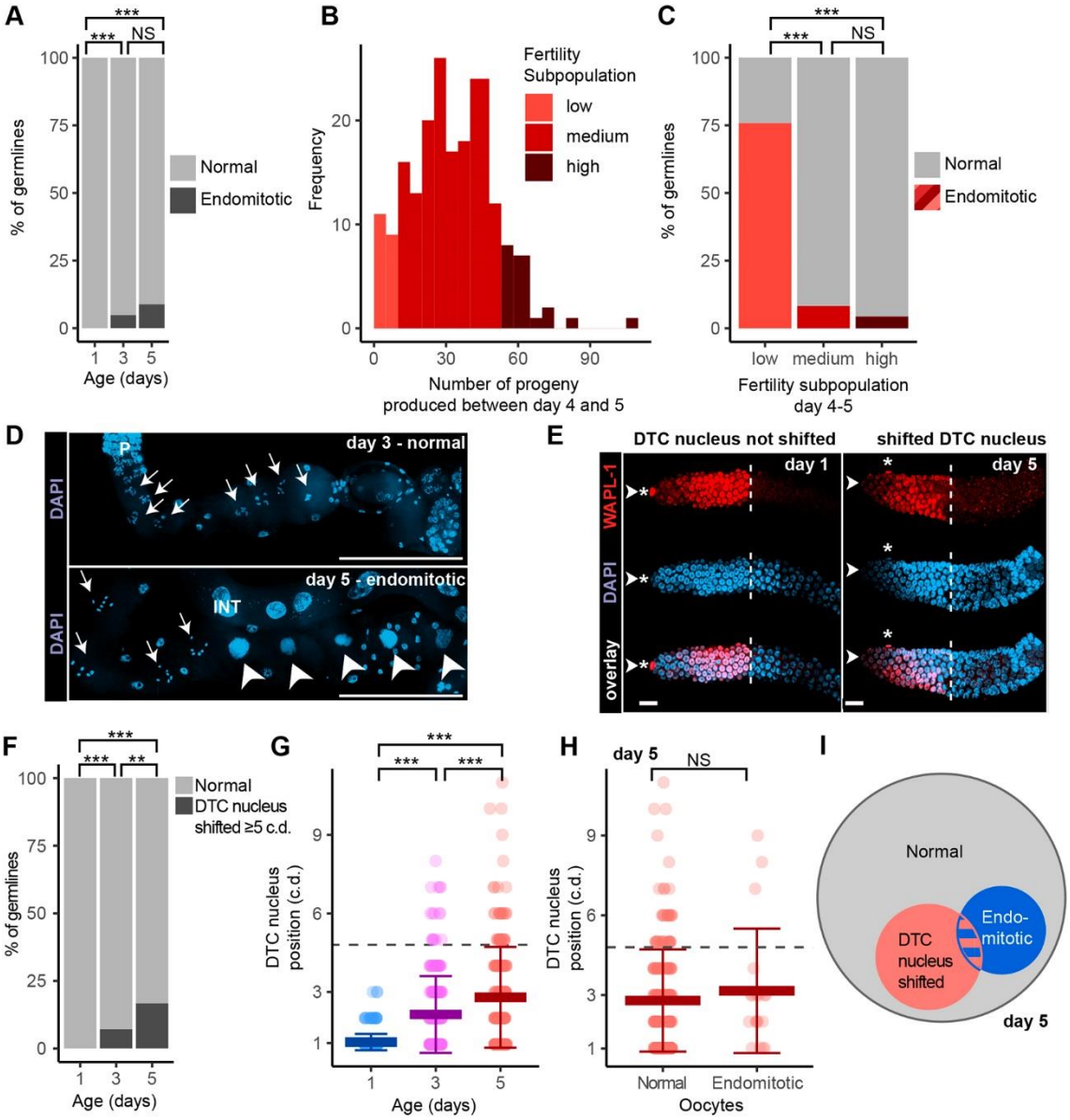


**Fig. 2: Endomitotic oocytes and a shifted DTC nucleus occurred at a low frequency.**
**A)** Day 1, 3 and 5 mated wild-type hermaphrodites were analyzed for endomitotic oocytes in dissected germlines. Gray indicates no detectable endomitotic oocytes (normal), and black indicates one or more endomitotic oocytes. PC test.
**B)** Longitudinal experiment - bars represent number of mated hermaphrodites (frequency) that produced the indicated number of progeny between days 4 and 5. We defined three fertility subpopulations: low (bottom 10%), medium (middle 80%), and high (top 10%).
**C)** Proportion of endomitotic germlines at day 5 in fertility subpopulations.
**D)** Representative fluorescence micrographs of normal diakinesis oocytes (arrows) in a day 3 adult (top) and endomitotic oocytes (arrowheads) in a day 5 adult (bottom), with DNA stained by DAPI. P, pachytene. INT, intestine. Scale bar = 20 μm.
**E)** Representative fluorescence micrographs of day 1 and 5 adult germlines stained for WAPL-1 (red, row 1), DAPI (blue, row 2), and WAPL-1+DAPI (row 3). Arrowhead indicates the distal

Development • Accepted manuscript

tip of the gonad, asterisk indicates the position of the DTC nucleus. The DTC nucleus is at cell diameter position 1 (left) and 5 (right). Dashed lines indicate the boundary of WAPL-1-positive cells. Scale bar=10μm.

**F,G)** DTC nucleus position was determined by counting the number of c.d. from the gonad tip in day 1, 3, and 5 mated hermaphrodites. **F)** gray indicates DTC nucleus was ≤4 c.d. (normal), black indicates the DTC nucleus was ≥5 c.d. (shifted) from the tip. PC test. **G)** each data point indicates position of one DTC nucleus. Position 1 means DTC nucleus is at the distal tip. KW test. Dashed line represents cutoff for panel **F**.

**H)** We categorized day 5 adult mated hermaphrodite germlines as non-endomitotic (normal) or endomitotic, and each data point indicates the position of one DTC nucleus. KW test.

**I)** Venn diagram, proportion of day 5 mated hermaphrodite germlines showing endomitotic nuclei (blue), shifted DTC nucleus (red), both (blue/red) or neither (gray). (See Supplemental Table 2 for statistics; NS indicates P>0.05, * P<0.05, ** P<.001, *** P<.0001.)

Development • Accepted manuscript

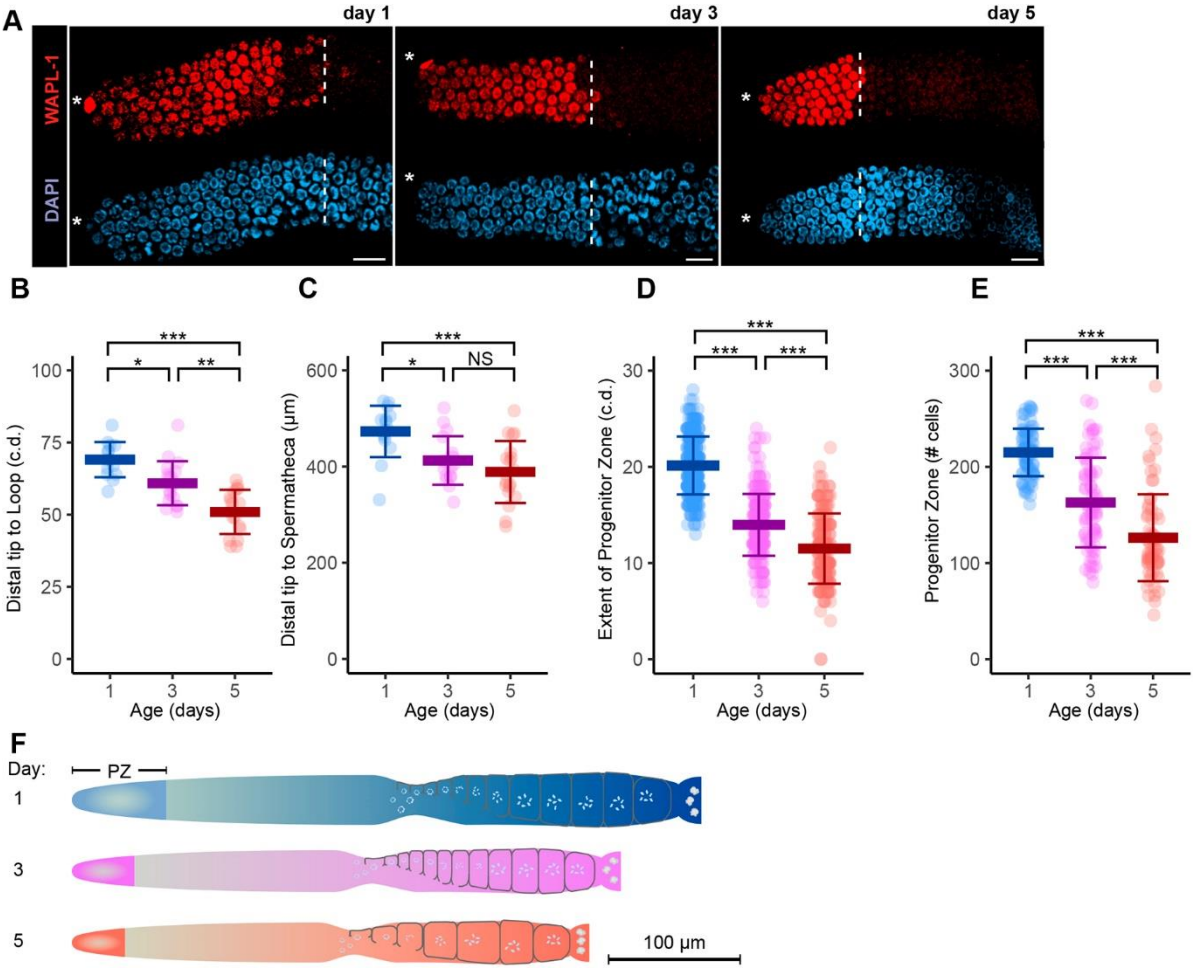


**Fig. 3: Population-wide, age-related decreases in the size of the germline and progenitor zone.**

**A)** Representative fluorescence micrographs of one germline from day 1, 3 and 5 adults stained for WAPL-1 (top, red) and DAPI (bottom, blue). Asterisks, DTC nucleus position; white dashed line, proximal boundary of WAPL-1-positive cells. Scale bar=10µm.

**B,C)** Each data point is length from the distal tip to the loop (in cell diameters, c.d.) (**B**) or spermatheca (in micrometers, used due to unequal size of cells in proximal region) (**C**) in mated hermaphrodites at adult days 1, 3 or 5. KW test.

**D)** Each data point is length of the PZ (in c.d.), defined by WAPL-1 antibody staining and measured from the distal tip to the last row where at least half of the cells were WAPL-1-positive. KW test.

**E)** Each data point is the total number of PZ cells, defined as WAPL-1-positive. KW test. (See Supplemental Table 3 for statistics)

**F)** Diagram of the size of the entire germline and PZ in day 1, 3, and 5 adults.

Development • Accepted manuscript

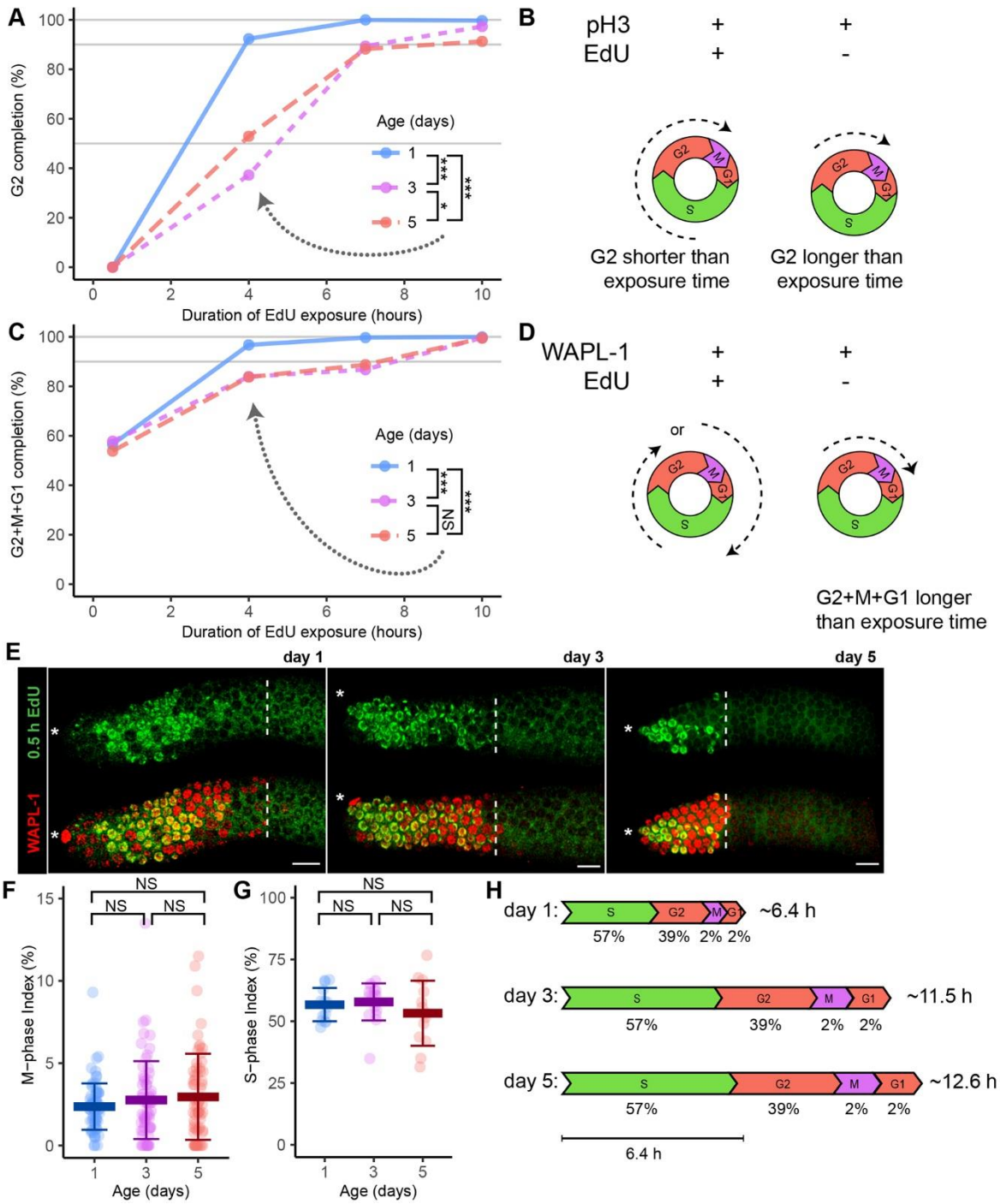


**Fig. 4: Population-wide, age-related increase in the duration of the cell cycle.**
Mated hermaphrodites at day 1 (blue), 3 (purple) or 5 (red) were exposed to EdU for 0.5, 4, 7, or 10 hours, and germlines were dissected and stained with anti-pH3 antibody, anti-WAPL-1 antibody, and/or EdU click chemistry.
**(A)** Percent G2 completion was defined as the number of cells that were both pH3-positive (indicative of M-phase) and EdU-positive (indicative of cell in S-phase sometime during EdU exposure), divided by the total number of pH3-positive cells. These data were used to estimate the median time taken to complete G2-phase (n=1655 cells, 366 germlines). Gray horizontal

Development • Accepted manuscript

lines indicate the 50th, 90th, and 100th percentiles. A PC test was used to compare the 4 hour time point (dotted arrow).

**B,D)** Dashed arrows in diagrams illustrate inferred cell cycle stage at the beginning (S or G2) and end (M, G1 or S) of the experiment.

**C)** Percent G2+M+G1 completion was defined as the number of cells that were both WAPL-1-positive (interpreted as being in the PZ) and EdU-positive, divided by the total number of WAPL-1-positive cells. These data were used to estimate the maximum time taken to complete G2+M+G1 phase (n=193 animals, 31958 cells). Gray horizontal lines indicate the 90th and 100th percentiles. A PC test was used to compare the 4 hour time point.

**E)** Representative fluorescence micrographs of one germline from adults exposed to EdU for 0.5 hours and stained for EdU (green, row 1), and EdU and WAPL-1 (red, yellow overlap, row 2). Asterisk, DTC nucleus position; white dashed line, proximal boundary of WAPL-1-positive cells. Scale bar=10μm.

**F)** Each data point indicates the M-phase index (number of cells that were pH3-positive divided by the number of PZ WAPL-1-positive cells).

**G)** Each data point indicates the S-phase index (number of EdU-positive cells divided by the number of PZ WAPL-1-positive cells) of adults following an EdU exposure of 0.5 hours. KW test. (See Supplemental Table 4 for statistics)

**H)** Scale diagrams illustrate the inferred duration of each cell cycle phase, values below indicate percent, and values at right indicate total duration. Scale bar=6.4 hours.

Development • Accepted manuscript

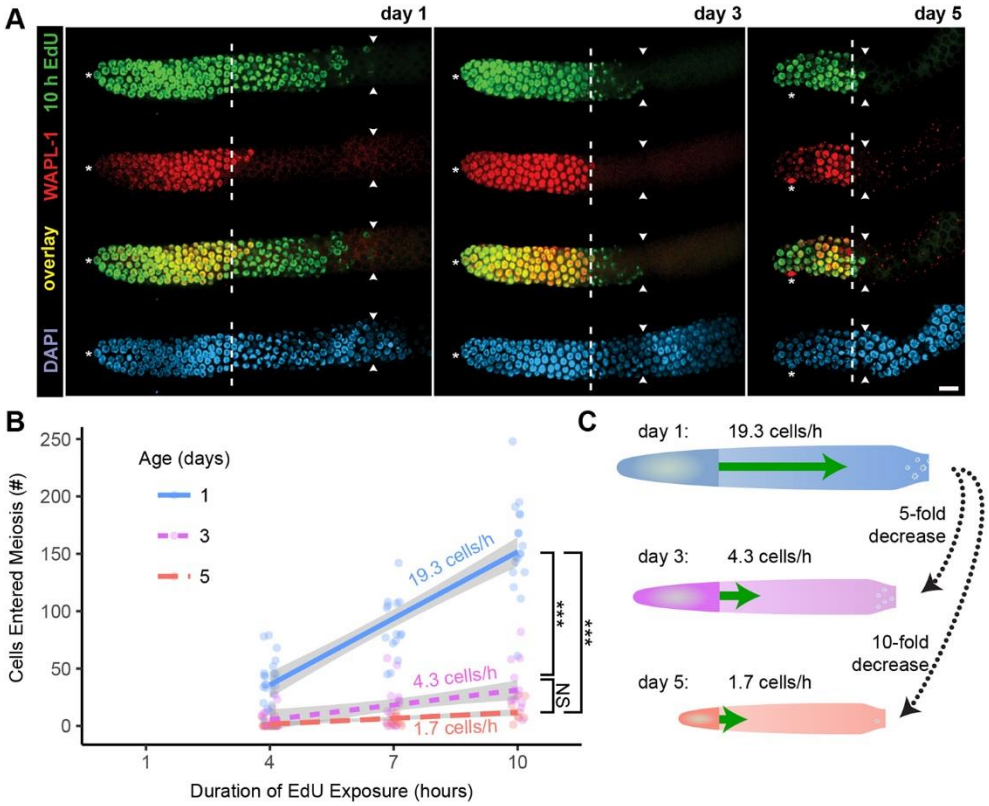


**Fig. 5: Population wide, age-related decrease in the rate of meiotic entry**

Mated hermaphrodites at day 1 (blue), 3 (purple), or 5 (red) were exposed to EdU for 4, 7, or 10 hours, and germlines were dissected and stained with anti-WAPL-1 antibody and EdU click chemistry.

**A)** Representative fluorescence micrographs of one germline from day 1, 3 and 5 adults exposed to EdU for 10 hours and stained for EdU (green, row 1), WAPL-1 (red, row 2), EdU+WAPL-1 (overlay, row 3) and DAPI (blue, row 4). Asterisk, DTC nucleus position; white dashed line, proximal boundary of WAPL-1-positive cells; and white arrowheads, proximal boundary of EdU-positive cells. Scale bar=10μm.

**B)** The rate of meiotic entry (cells/hour) was calculated from the slope of the linear regression of the number of cells that entered meiosis (EdU-positive, WAPL-1-negative) versus the duration of the EdU exposure. Gray range indicates 95% confidence interval on linear regression. KW test compared the number of cells entered meiosis in 10 hours. (See Supplemental Table 5 for statistics)

**C)** Diagram of day 1, 3, and 5 germlines highlighting the age-related decrease in the rate of meiotic entry (green arrows).

Development • Accepted manuscript

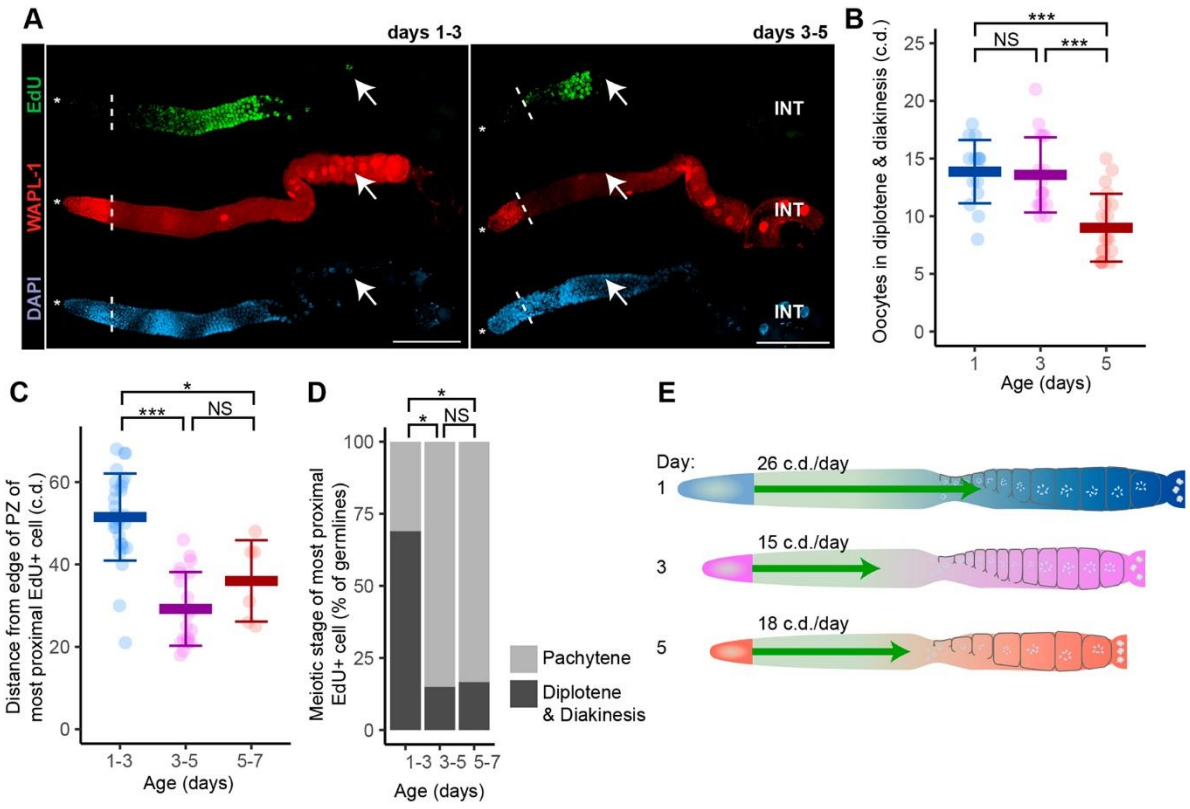


**Fig. 6: Population-wide, age-related decrease in the rate of meiotic progression**
Mated hermaphrodites at days 1, 3 or 5 were fed EdU labeled bacteria for 4 hours ("pulse") to label all cells that underwent S-phase and then fed unlabeled bacteria for 48 hours ("chase") to determine the extent of movement. Because the distance is measured during a two-day interval, the rate is an average of the rate during days 1-3, 3-5, or 5-7.

**A)** Representative fluorescence micrographs of one germline labeled at day 1 and 3 and analyzed after 48 hours by staining for EdU (green, row 1), WAPL-1 (red, row 2), and DAPI (blue, row 3). Asterisk, DTC nucleus position; white dashed line, proximal boundary of WAPL-1-positive cells; white arrows, proximal boundary of EdU-positive cells; and INT, intestine. Scale bar=100μm.

**B)** Each data point represents the number of cell diameters of diplotene and diakinesis oocytes in the proximal assembly-line in mated hermaphrodites at adult days 1, 3 or 5. KW test.

**C)** In each germline, the most proximal EdU-positive cell was identified, and each data point indicates its distance in c.d. from the proximal edge of the PZ. Because the most proximal EdU-positive cell was presumably near the proximal end of the PZ at the beginning of the experiment, this value estimates the distance moved during 48 hours. KW test.

**D)** In each germline, the most proximal EdU-positive cell was categorized as pachytene or diplotene/diakinesis. PC test. (See Supplemental Table 6 for statistics)

**E)** Diagram of day 1, 3, and 5 germlines highlighting the age-related decrease in the rate of meiotic progression (green arrows).

Development • Accepted manuscript

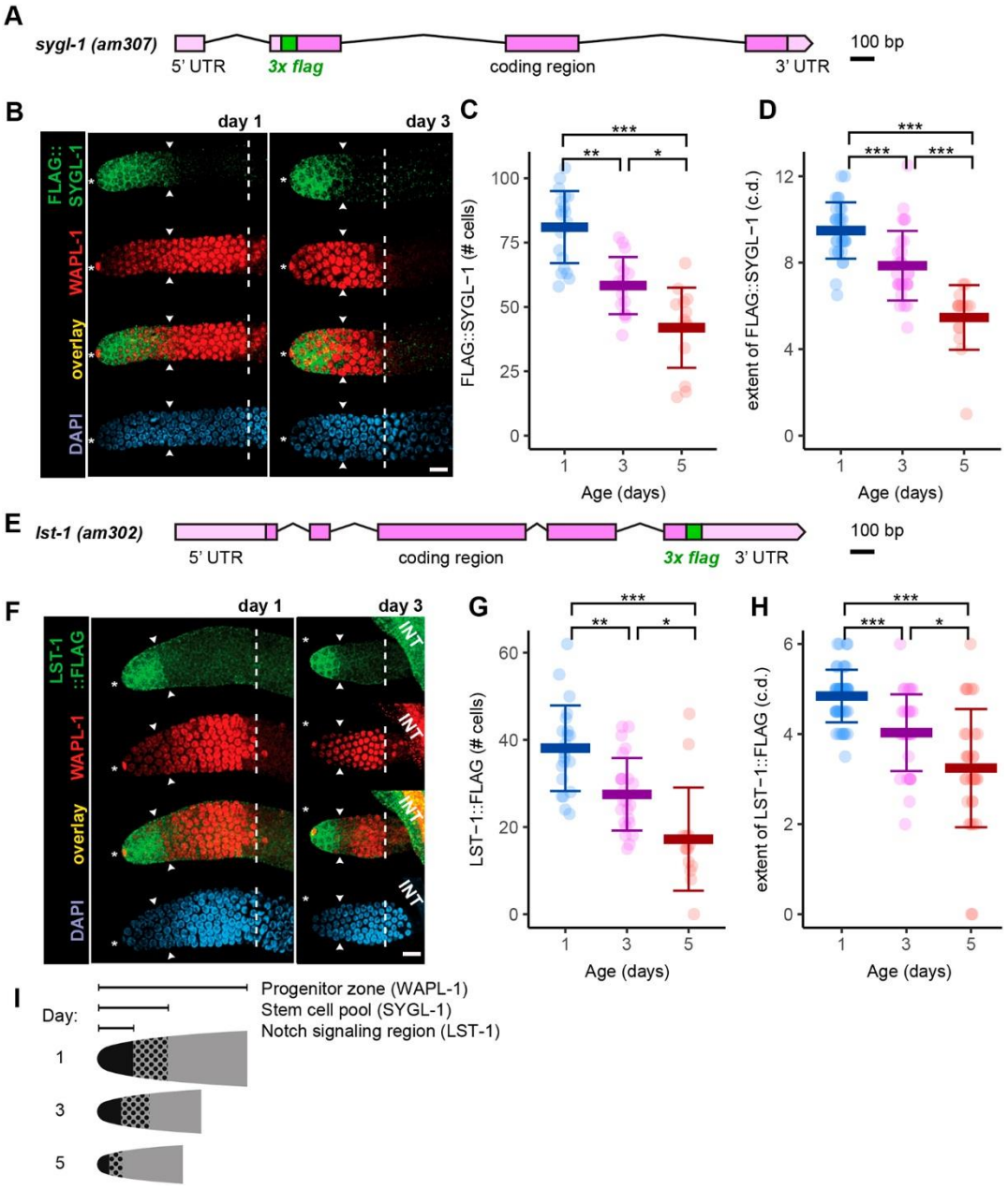


**Fig. 7: Population-wide, age-related decrease in the stem cell pool and GLP-1 (Notch) signaling.**

Mated *sygl-1(am307)* and *lst-1(am302)* hermaphrodites expressing FLAG::SYGL-1 or LST-1::FLAG fusion proteins, respectively, were stained with anti-FLAG antibody.

**A,E)** Diagram of the *sygl-1(am307)* and *lst-1(am302)* genomic loci. DNA encoding 3xFLAG epitopes was inserted in-frame using CRISPR/Cas9 genome editing, resulting in an N-terminally (**A**, *sygl-1*) or a C-terminally (**E**, *lst-1*) tagged fusion protein expressed from the endogenous locus.

**B, F)** Representative fluorescence micrographs of one germline from day 1 and 3 adults stained for

FLAG::SYGL-1 (**B**) or LST-1::FLAG (**F**) (green, row 1), WAPL-1 (red, row 2), FLAG+WAPL-1 (overlay, row 3) and DAPI (blue, row 4). Asterisks, DTC nuclear position; white arrowheads, proximal boundary of FLAG staining; white dashed lines, boundary of WAPL-1-positive cells; and INT, intestine. Scale bar=10μm.

Development • Accepted manuscript

**C,D,G,H)** Data points indicate the number of expressing cells (**C**,**G**) or the extent of these cells (c.d.) (**D**,**H**). KW test. (See Supplemental Table 7 for statistics)
**I)** Diagram of the size decrease in the PZ, stem cell pool, and Notch signaling region.

Development • Accepted manuscript

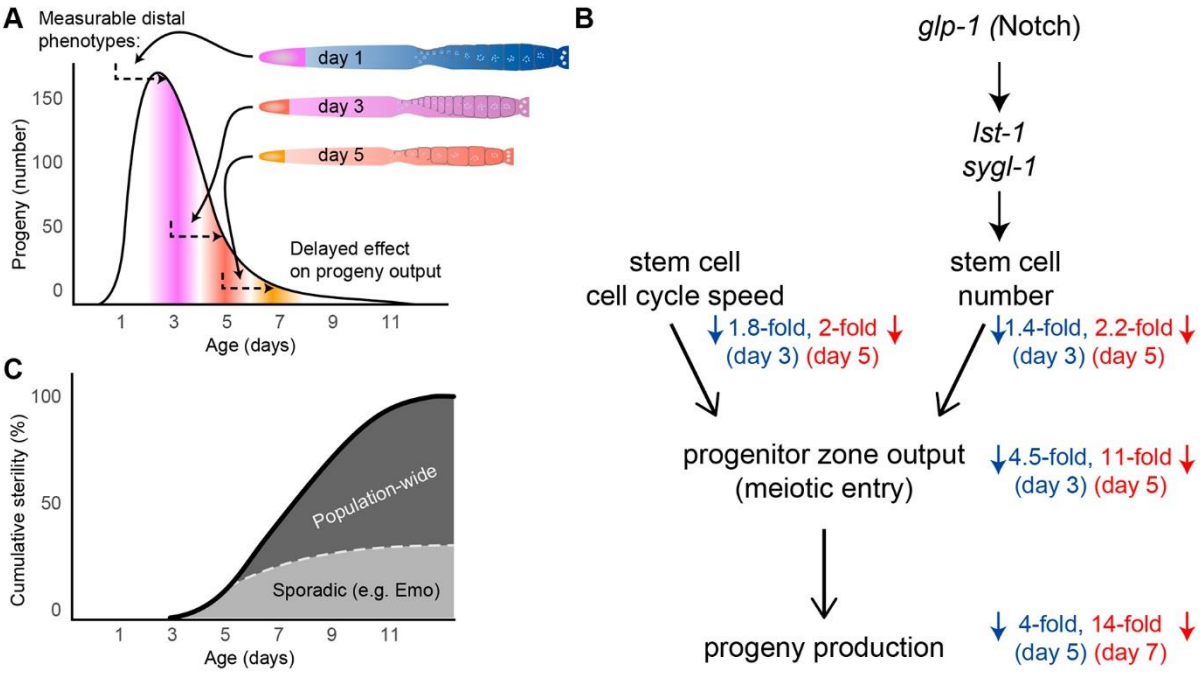


**Fig. 8: Model of age-related changes that drive reproductive decline in sperm-replete *C. elegans*.**

**A)** Diagrams of day 1, 3, and 5 germlines are shown with a typical wild-type progeny production curve (like in **Fig.1A**) to illustrate that PZ cells take two or more days to become oocytes and be laid as eggs. Thus, age-related changes in the PZ of day 3 and 5 adults affect egg laying on days 5 and 7, respectively.

**B)** A model relating *glp-1* (Notch) activity and cell cycle dynamics to progeny production. Filled arrows indicate molecular pathway, line arrows indicate cell events from distal (top) to proximal (bottom). Blue and red numbers indicate fold-declines in function between peak and days 3, 5, and 7.

**C)** The cumulative sterility of a population results from age-related changes that are both sporadic and population-wide. The dotted line indicates a projection of the relative contribution of sporadic defects (e.g. endomitotic oocytes) as a cause of sterility. Population-wide declines in stem cell number and activity contribute to the quantitative decline in progeny production in all animals and are the cause of sterility in a fraction of the population.

Development • Accepted manuscript

**Table 1: CRISPR/Cas9 plasmids and oligonucleotides specific to this study**

| Locus | Corresponding Plasmid | Oligo name | Sequence | Notes |
|---|---|---|---|---|
| *lst-1* | pZK07 | ZK034 | TTTGGAAGAACATTTGAAGGGGG | g4 |
| | pZK07 | ZK035 | AAACCCCCCTTCAAATGTTCTTC | g4 |
| | pZK13 | ZK073 | TTTGTTGCTCAACTCGATCGTGC | g16 |
| | pZK13 | ZK074 | AAACGCACGATCGAGTTGAGCAA | g16 |
| | NA | ZK038 | AAAAATCTTCTCAAATTATTATTATTTCAGATGT CCCCGTTTATGGTTCGCTCAATTGGACCGAGCA GGTTCAGAGATGGTGGAGCAGATGGGACACG CTCGAAATGTTCCAGTCGACTACAAAGACCATG ACGGTGATTATAAAGATCATGATATCGATTACA AGGATGACGATGACAAGTAAGCAATAAAATTG GTTTAAATATCAATTAATTTATATTTTACGACCC GCTTGAATAGTTCTTCTTGTTTTACACTATCATC CAAAAAAATGCGGTTC | gblock |
| | NA | ZK039 | AAAAATCTTCTCAAATTATTATTATTTCAGA | amplify gblock |
| | NA | ZK040 | GAACCGCATTTTTTTTGGATG | amplify gblock |
| | NA | ZK028 | CACTTTATGATATGCAAGGACGAG | genotyping |
| | NA | ZK029 | CAAAAGAGCACATGGATATACAGC | genotyping |
| *sygl-1* | pZK15 | ZK041 | TTTGGACGTCAGAGACGATGAGG | g1 |
| | pZK15 | ZK042 | AAACCCTCATCGTCTCTGACGTC | g1 |
| | pZK17 | ZK043 | TTTGTGGAATGGCATTATGCACG | g5 |
| | pZK17 | ZK044 | AAACCGTGCATAATGCCATTCCA | g5 |
| | pZK20 | ZK045 | TTTGAACTCTACATGGATCACCG | g6 |
| | pZK20 | ZK046 | AAACCGGTGATCCATGTAGAGTT | g6 |
| | NA | ZK049 | TTCAGCGATCATCGAACCATTGTCATCACGCCA CGTGCATAATGGACTACAAAGACCATGACGGT GATTATAAAGATCATGATATCGATTACAAGGAT GACGATGACAAGCCATTCCATTATCCAAAATTA TATATGGACCATCGCGGAAACATGTCTACGTCT TCGTCTCTGACGTCATCGACAACCGCCACGTCA TCA | repair oligo |
| | NA | ZK047 | ATCTACCCGCCGATTTTCTAAT | genotyping |
| | NA | ZK048 | ATCTCCAAGTGTTGCACATAACC | genotyping |

Development • Accepted manuscript

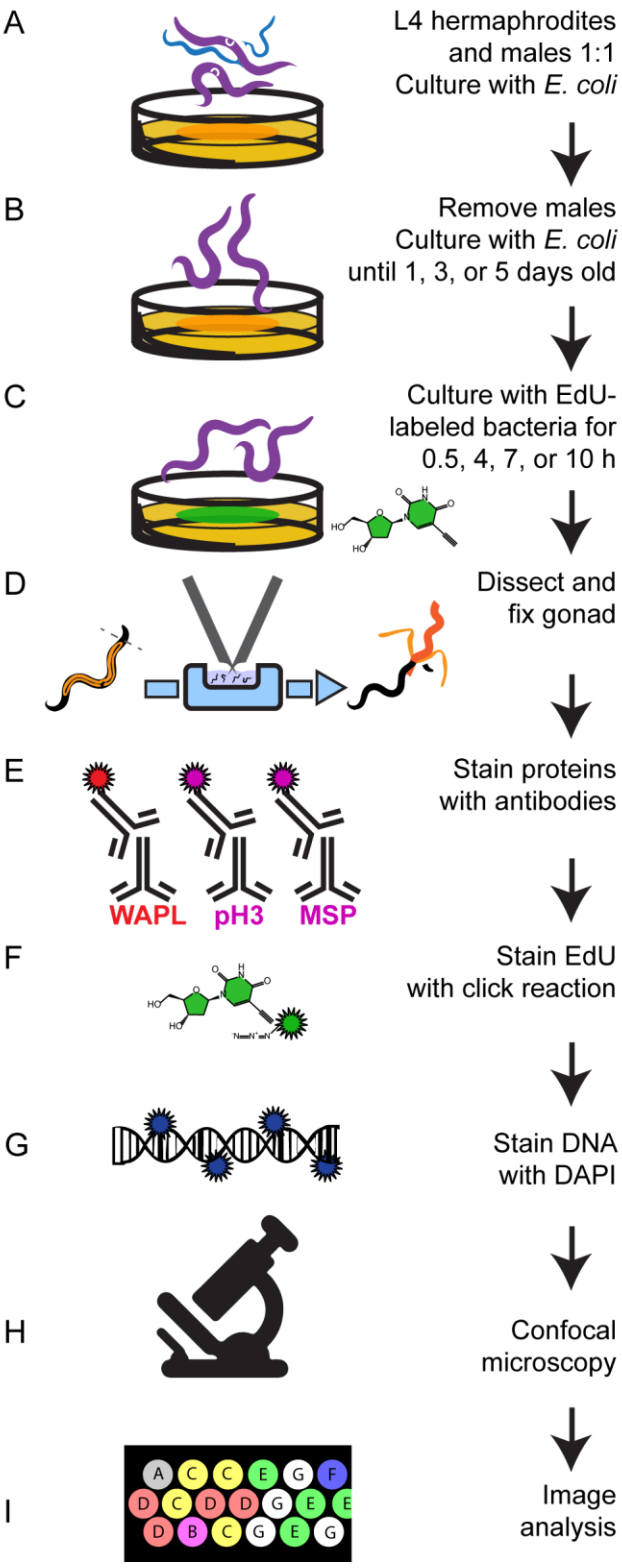


Development • Supplementary information

**Figure S1. Experimental Workflow.**

Experimental workflow used to assay the relationship between S-phase (EdU labeling), M-phase (pH3 antibody staining), progenitor zone cells, as well as the somatic gonadal DTC and sheath cell nuclei (WAPL-1 antibody staining), sperm presence (Major Sperm Protein antibody staining), and DNA morphology of each individual *C. elegans* germline. Hermaphrodites were mated to males **(A)**, cultured to the appropriate age **(B)**, EdU labeled by feeding **(C)**, dissected **(D)**, and stained with antibodies **(E)**. A click reaction was used to attach a dye to EdU **(F)**, DNA was stained with DAPI **(G)**, and germlines were imaged on a spinning disc confocal microscope **(H)** and analyzed in FIJI **(I)**. Diagram modified with permission from Kocsisova et al. (2018a).

Development • Supplementary information

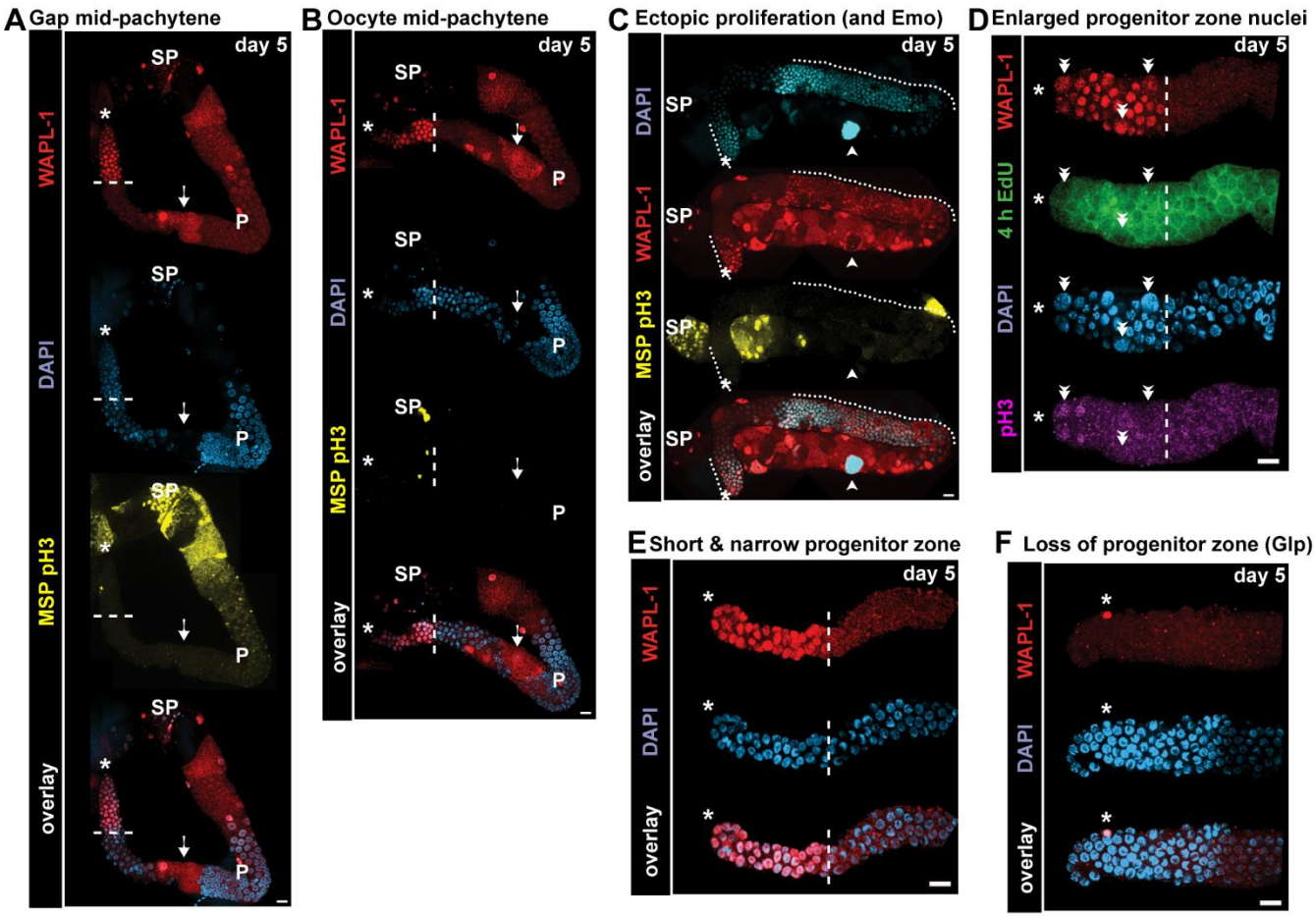


**Figure S2. Very low frequency germline defects displayed by day 5 mated hermaphrodites.** Representative confocal fluorescence micrographs of germlines displaying defects observed at very low frequency in mated day 5 wild-type hermaphrodites. Germlines were stained for WAPL-1 (red), DAPI (blue), MSP (Major Sperm Protein) and pH3 (both yellow), EdU (green), pH3 (violet), or a combination of markers (overlay). Asterisk indicates the position of the DTC nucleus, and white dashed line indicates the proximal boundary of WAPL-1-positive cells. P indicates pachytene region. SP indicates sperm in spermatheca. Scale bar = 10 μm **(A)** Arrow points to a gap in the middle of the pachytene region that lacks germ cell nuclei. **(B)** Arrow points to oocyte-like formations in the middle of the pachytene region. **(C)** Ectopic proliferation indicated by two WAPL-1-positive regions, one at the normal distal position and another more proximal, highlighted by dotted white lines; this germline also contained an endomitotic oocyte in the proximal germline, indicated with an arrowhead. **(D)** Double arrowheads indicate enlarged progenitor zone nuclei, suggestive of a mitotic cell cycle abnormality. **(E)** A germline that displayed an unusually short and narrow progenitor zone. **(F)** Apparent premature meiotic entry (Glp) phenotype, as the distal germline lacks WAPL-1-positive cells; note that DTC nucleus (asterisk) is displaced 7 c.d. from the distal end and may be nonfunctional.

Development • Supplementary information

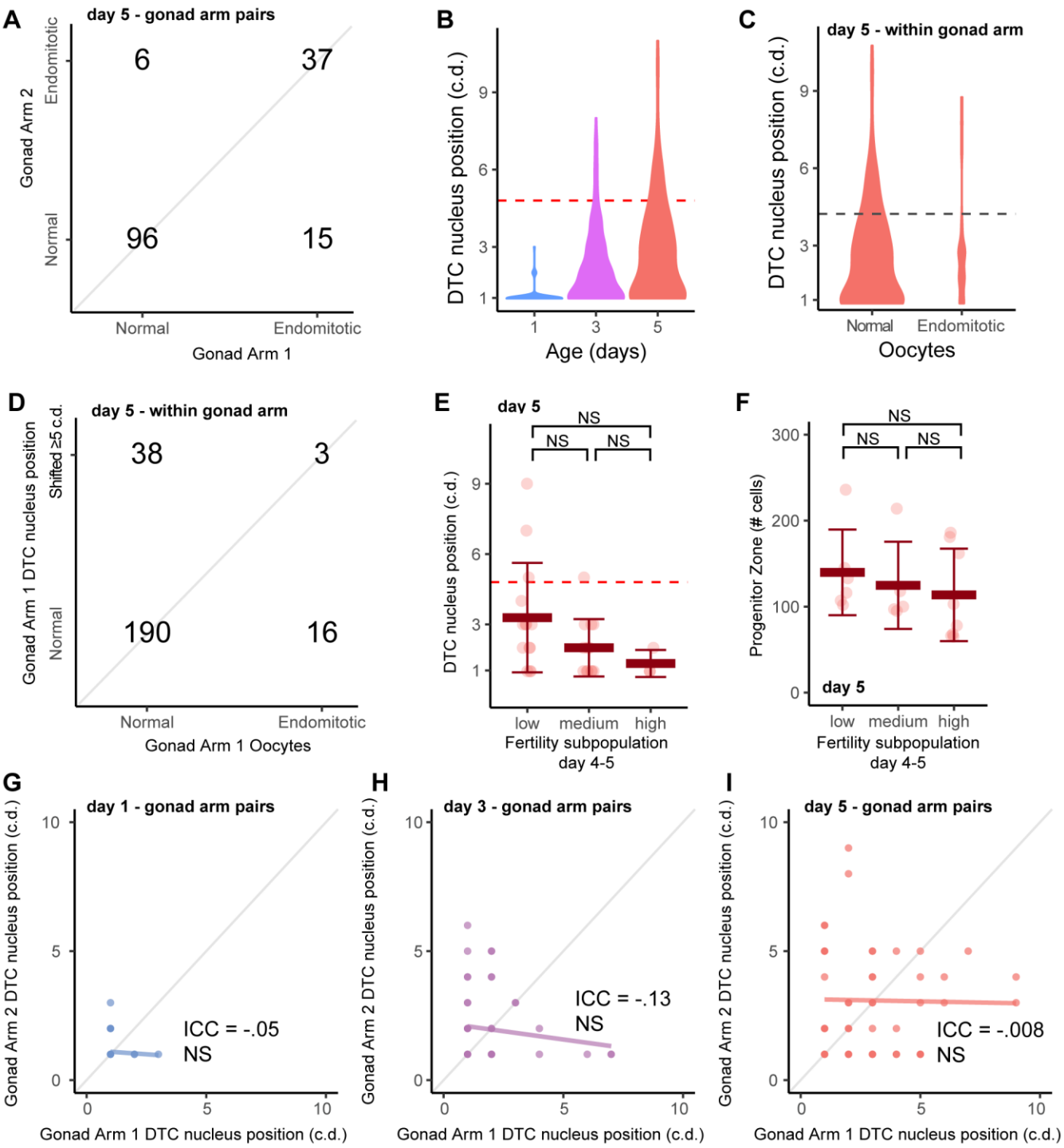


**Figure S3. Endomitotic oocytes and a shifted DTC nucleus occurred at a low frequency.**
**A)** To investigate co-occurrence of endomitotic oocytes in the two gonad arms in day 5 adults, we took advantage of a subset of animals in which both gonad arms were visible after dissection by comparing within-pair variation to between-pair variation using an intraclass correlation analysis. 96 animals displayed two normal germlines, 37 animals displayed two Emo germlines, and 21 animals displayed discordant germlines. There was a significant intraclass correlation (intraclass correlation coefficient = 0.68, P<.0000001). This result indicates the existence of a systemic process that uncouples oocyte meiotic

Development • Supplementary information

maturation from ovulation, leading to the generation of endomitotic oocytes in both gonad arms in a small number of animals.

**B)** Violin plots show the distribution of the position of the DTC nucleus (in cell diameters, c.d.) in day 1, 3 and 5 mated hermaphrodites. The same data are displayed in **Fig.2G**. The DTC nucleus was identified by its position at the exterior of the distal gonad and bright WAPL-1 staining, and its position was determined by counting the number of cell diameters from the tip of the gonad.

**C)** Violin plots show the distribution of the position of the DTC nucleus in day 5 mated hermaphrodites in germlines with and without endomitotic oocytes. The same data are displayed in **Fig.2H**.

**D)** To investigate co-occurrence of endomitotic oocytes and a shifted DTC nucleus, we categorized day 5 mated wild-type hermaphrodites as (i) not displaying endomitotic nuclei (normal) or displaying endomitotic nuclei, and (ii) not displaying a shifted DTC nucleus (<5 c.d., defined as normal) or displaying a shifted DTC nucleus (≥5 c.d., defined as shifted). 190 animals displayed two normal germlines, 3 animals displayed an Emo germline and a shifted DTC nucleus, and 54 animals displayed discordant germlines. There was not a significant relationship between endomitotic oocytes and shift of the DTC nucleus (Pearson's Chi-squared $P>0.99$), indicating one systemic process does not cause both defects.

**E)** Each data point indicates the position of one DTC nucleus in the three fertility subpopulations of day 5 animals defined in **Fig.2B** (n=14, 13, 3). Bars represent the average, and whiskers represent the standard deviation. Position 1 means the DTC nucleus is at the distal tip. Dashed line represents cutoff for a nucleus to be designated as "shifted". Comparison by Kruskal-Wallis test. The position of the DTC nucleus at day 5 did not correlate with the number of progeny produced between day 4 and 5.

**F)** Each data point indicates the size of the progenitor zone measured as total number of cells in the three fertility subpopulations of day 5 animals defined in **Fig.2B**. Bars represent the average, and whiskers represent the standard deviation. Comparison by Kruskal-Wallis test. The size of the progenitor zone at day 5 did not correlate with the number of progeny produced between day 4 and 5.

**E,F)** We hypothesize that an effect of the shifted DTC nucleus and progenitor zone size on progeny production would be delayed by 2-3 days, as cells in the distal germline require 2-3 days to progress through meiosis, mature, be ovulated, fertilized, and deposited. Thus, the absence of a correlation was expected, and does not rule out the possibility that changes in distal germline morphology affect progeny production on later days that could not be measured in this experiment.

**G-I)** To investigate correlation of the DTC nucleus position in the two gonad arms in day 1, 3, and 5 adults, we took advantage of a subset of animals in which both gonad arms were visible after dissection by comparing the within-pair variation to the between-pair variation using an intraclass correlation analysis. There was no significant correlation in the degree of DTC nucleus shift within a pair of germlines in the same animal. Thus, the shifted DTC nucleus appears to result from local rather than systemic conditions. NS indicates $P>0.05$, * $P<0.05$, ** $P<.001$, *** $P<.0001$. (See Supplemental Table S3 for statistics)

Development • Supplementary information

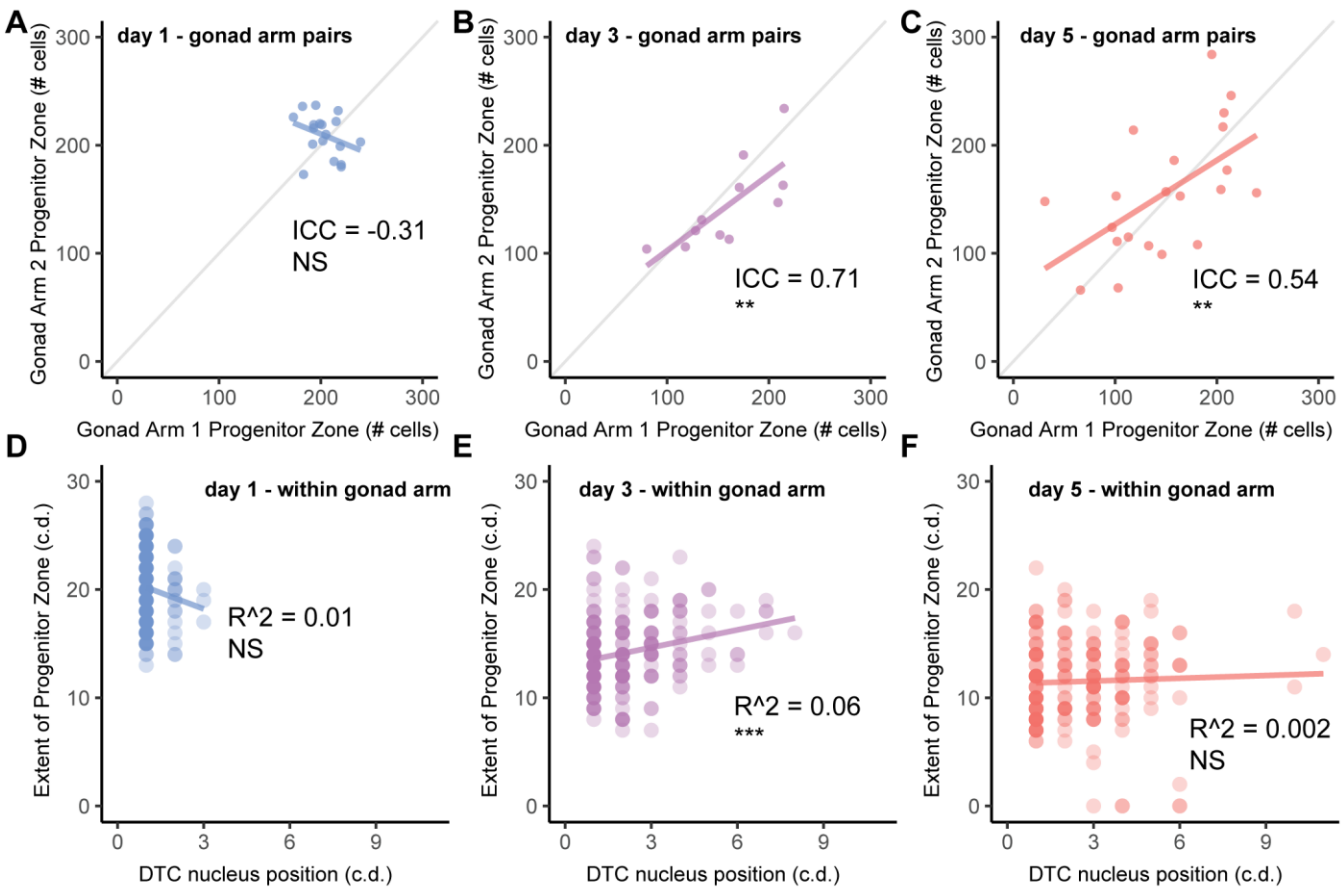


**Figure S4. Correlational analysis of distal phenotypes**

**A-C)** To investigate the relationship between the progenitor zone size in the two gonad arms in day 1, 3, and 5 adults, we took advantage of a subset of animals in which both germlines were visible after dissection by comparing the within-pair variation to the between-pair variation using an intraclass correlation analysis. Each data point indicates total number of progenitor zone cells in the two gonad arms of one animal. The line is a best fit, and statistical comparisons are shown. These data indicate that the age-related decrease in progenitor size appears to be result from systemic conditions.

**D-F)** To investigate the relationship between the DTC nucleus position and the progenitor zone size in individual animals, we measured both values in the same gonad arm. Data points represent the two values expressed in cell diameters. There was no significant correlation in the degree of DTC nucleus shift and the extent of the progenitor zone in day 1 and 5 animals, and a slight positive correlation in day 3 animals. NS indicates P>0.05, * P<0.05, ** P<.001, *** P<.0001. (See Supplemental Table S4 for statistics)

Development • Supplementary information

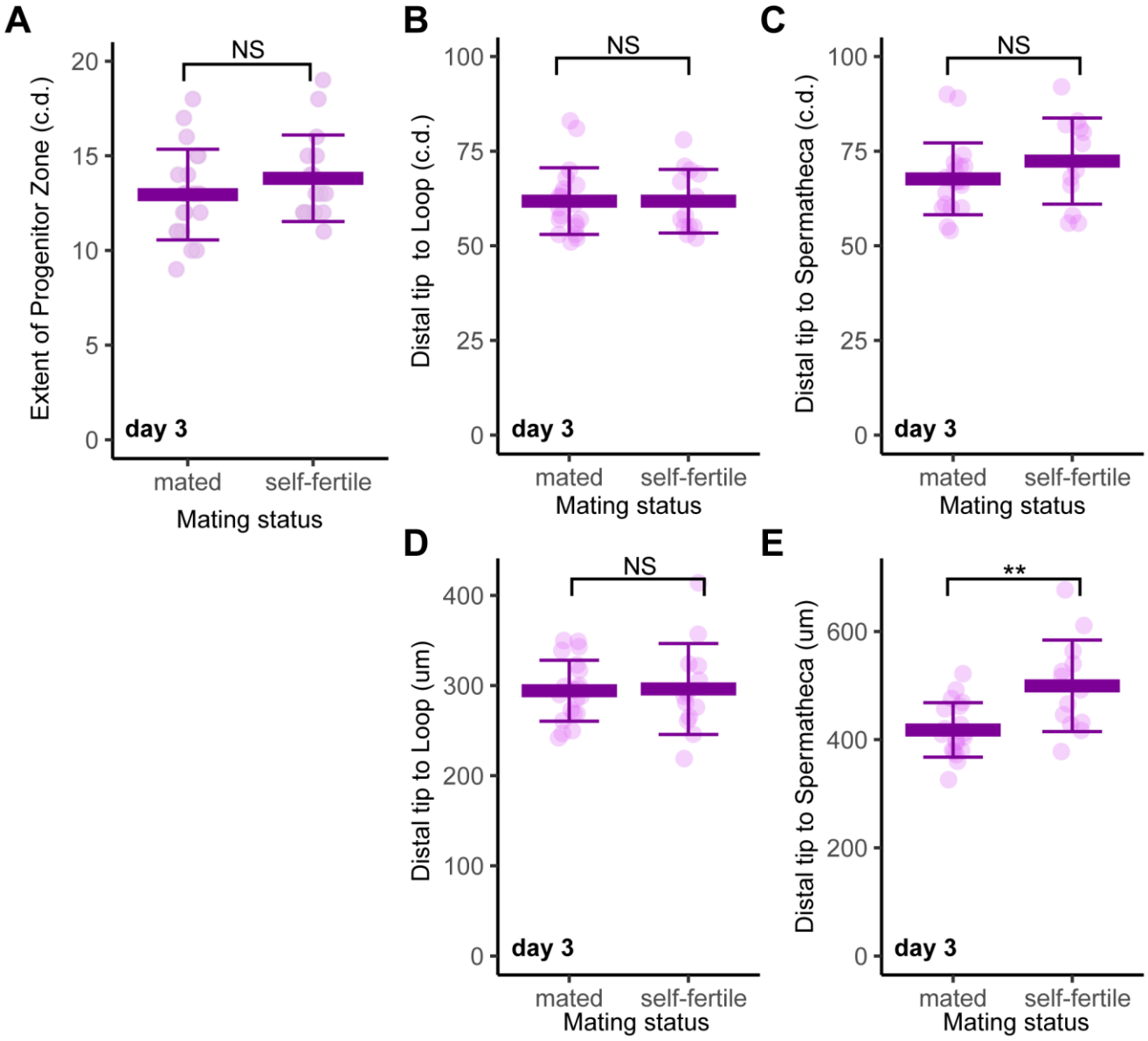


**Figure S5. Evaluation of the effect of male mating on hermaphrodite germline size**

To determine how mating influences the size of the germline, we analyzed day 3 adults that were self-fertile or mated to males for 24 hours. There was no significant difference in the length (measured in cell diameters) of the progenitor zone **(A)**, the distal germline **(B)**, or the entire germline **(C)** comparing self-fertile and mated animals. When the distal germline **(D)** or the entire germline **(E)** were measured using micrometers as the unit, the distal germline displayed no significant difference, whereas the entire germline was significantly longer in self-fertile animals. The likely reason for this difference is that some self-fertile hermaphrodites were sperm-depleted at day 3, resulting in diakinesis arrested oocytes that were stacked-up in the proximal germline, which extends the length of the tissue. NS indicates P>0.05, * P<0.05, ** P<.001, *** P<.0001. (See Supplemental Table S5 for statistics)

Development • Supplementary information

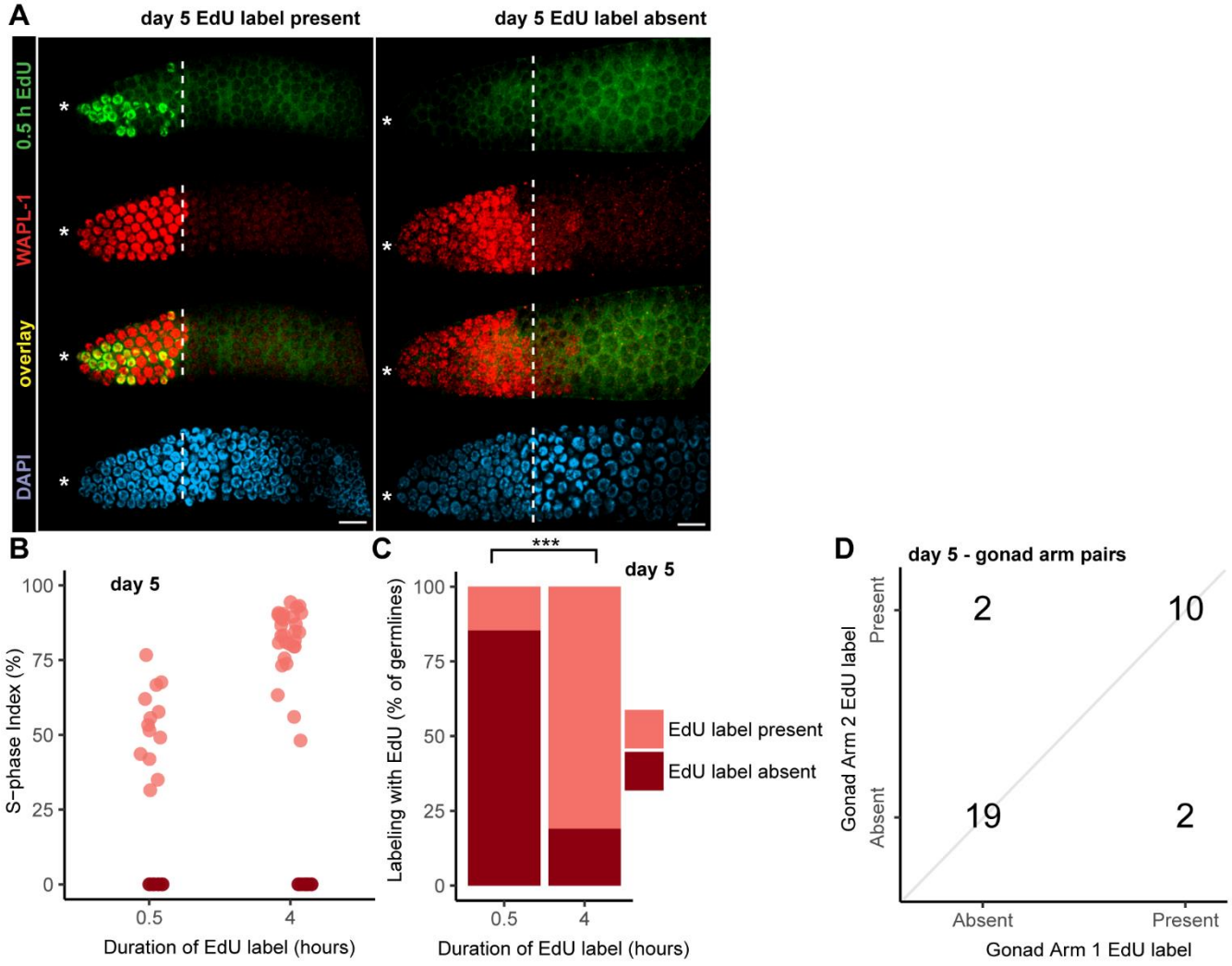


**Figure S6. A fraction of sperm-replete day 5 animals displayed no EdU labeling.**

**A)** Representative fluorescence micrographs of two germlines from day 5 adults fed EdU for 0.5 hours and subsequently stained for EdU (green, row 1), WAPL-1 (red, row 2), EdU and WAPL-1 (row 3) and DAPI (blue, row 4). Panels on the left show an animal that successfully labeled with EdU; panels on the right show an animal that failed to label with EdU. Asterisks indicate the position of the DTC nucleus, and white dashed lines indicate the proximal boundary of WAPL-1-positive cells. Scale bar = 10 μm.

**B)** Each data point indicates the S-phase index (number of EdU positive cells divided by the number of progenitor zone WAPL-1-positive cells) of day 5 animals fed EdU for either 0.5 or 4 hours. Both data sets display a bimodal distribution.

**C)** The proportion of day 5 adults that labeled with EdU in 0.5 or 4 hours. Dark red indicates germlines with no detectable EdU labeled cells, and light red indicates germlines with multiple EdU labeled cells. n=130, 63; three or more biological replicates. Comparison by Pearson's Chi-squared test.

Development • Supplementary information

**D)** To investigate co-occurrence of EdU labeling in the two gonad arms in day 5 adults, we took advantage of a subset of animals in which both gonad arms were visible after dissection following feeding EdU for 0.5 h. 19 animals displayed two germlines lacking EdU labeling, 10 animals displayed two germlines positive for EdU labeling, and 4 animals displayed discordant germlines. There was a significant intraclass correlation (intraclass correlation coefficient=0.75, $p<0.0001$), suggesting a systemic cause of germline non-labeling. (See Supplemental Table S6 for statistics)

Development • Supplementary information

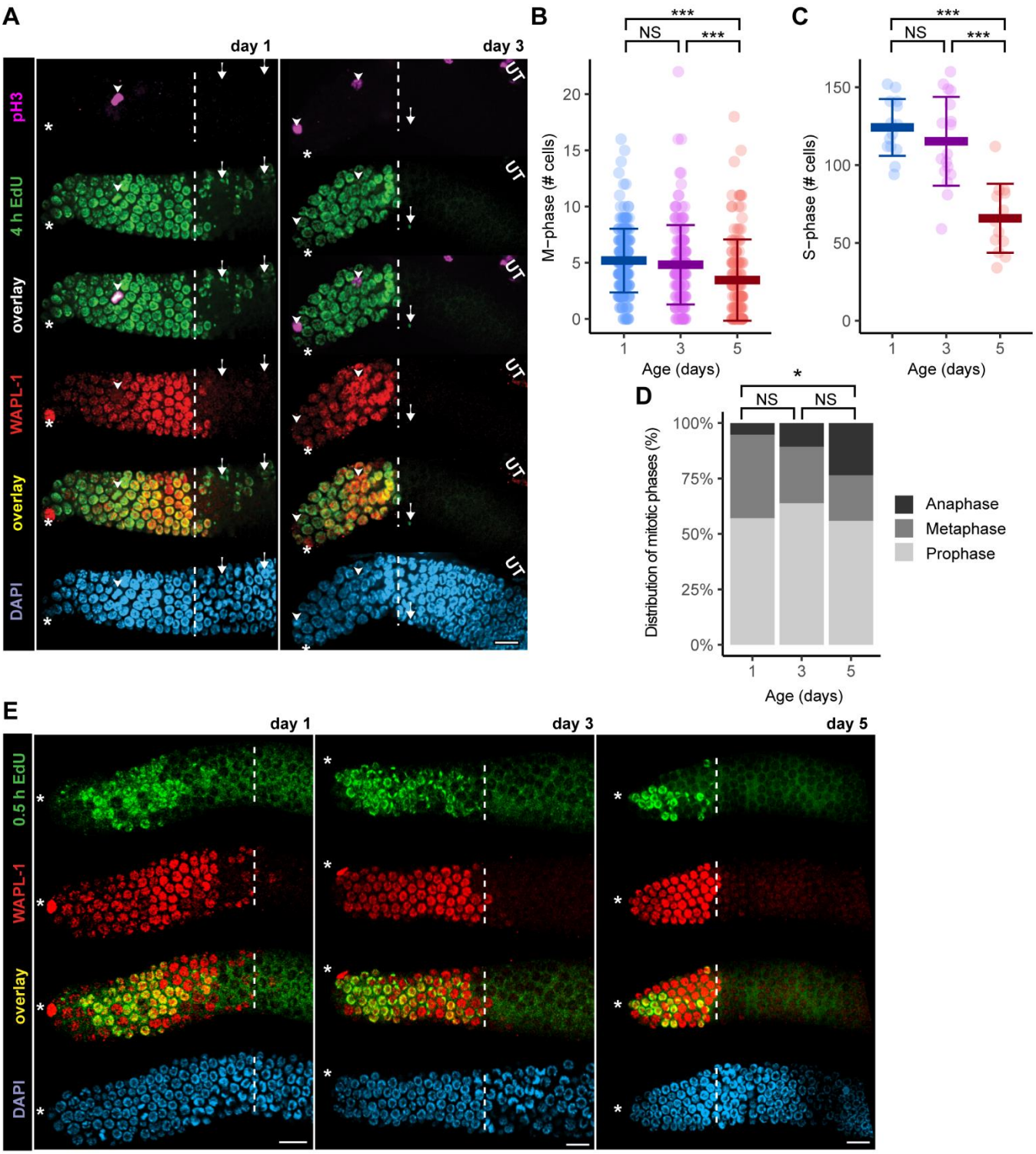


**Figure S7. Age-related change in the numbers of M-phase and S-phase cells.**

**A)** Representative fluorescence micrographs of germlines from day 1 (left) and day 3 (right) adults fed EdU for 4 hours and subsequently stained for pH3 (magenta, row 1), EdU (green, row 2), pH3 and EdU (overlay, row 3), WAPL-1 (red, row 4), EdU and WAPL-1 (overlay, row 5), and DAPI (blue, row 6). Asterisks indicate the position of the DTC nuclei, and white dashed lines indicate the proximal boundary of WAPL-1-

Development • Supplementary information

positive cells. Arrowheads indicate pH3-positive cells. Arrows indicate examples of EdU-positive, WAPL-1-negative cells. UT indicates the uterus, where Major Sperm Protein positive sperm are visible in magenta. Scale bar = 10 μm.

**B)** Each data point indicates the number of M-phase (pH3-positive) cells per gonad arm of day 1, 3, and 5 adults. Bars represent the average, and whiskers represent the standard deviation. n=213, 155, 134 in 4 or more biological replicates. Comparison by Kruskal-Wallis test.

**C)** Each data point indicates the number of S-phase (EdU-positive) cells per gonad arm of day 1, 3, and 5 adults fed EdU for 0.5 hours. Bars represent the average, and whiskers represent the standard deviation. n= 14, 17, 13 in two or more biological replicates. Comparison by Kruskal-Wallis test.

**D)** Distribution of mitotic phases among pH3 immunoreactive cells was determined by DAPI morphology in day 1, 3, and 5 adults and characterized as anaphase (black), metaphase (dark gray) or prophase (light gray). n=77, 47, 34. Comparison by Pearson's Chi-squared test. NS indicates $P>0.05$, * $P<0.05$, ** $P<.001$.

**E)** Representative fluorescence microscope images of germlines from day 1, 3, and 5 adults fed EdU for 0.5 hours and subsequently stained for EdU (green, row 1), WAPL-1 (red, row 2), EdU and WAPL-1 (overlay, row 3) and DAPI (blue, row 4). Asterisks indicate the position of the DTC nuclei, and white dashed lines indicate the proximal boundary of WAPL-1-positive cells. Scale bar = 10 μm. Some of these images appear in **Fig.3A** and **Fig.4E**. (See Supplemental Table S7 for statistics)

Development • Supplementary information

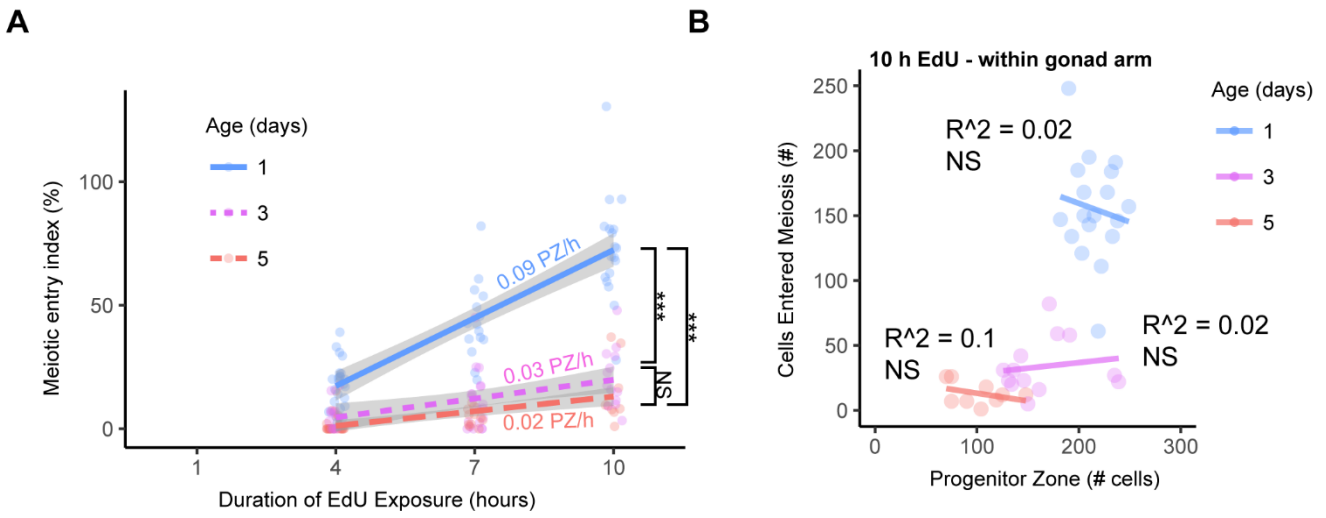


**Figure S8. Age-related decrease in the rate of meiotic entry**

**A)** Mated hermaphrodites at day 1 (blue), 3 (purple), or 5 (red) were exposed to EdU for 4, 7, or 10 hours, and germlines were dissected and stained with anti-WAPL-1 antibody and EdU click chemistry. The meiotic entry index was calculated by dividing the number of cells that entered meiosis (EdU positive, WAPL-1 negative) by the number of progenitor zone cells (WAPL-1-positive). The normalized rate of meiotic entry (% of progenitor zone per hour) was calculated from the slope of the linear regression of the meiotic entry index versus the duration of the EdU exposure. Gray range indicates 95% confidence interval on linear regression. Comparison by Kruskal-Wallis test compared the meiotic entry index at 10 hours. NS indicates P>0.05, *** P<.0001.

**B)** To investigate the relationship between the rate of cells entering meiosis and the progenitor zone size in individual animals, we measured both values in the same gonad arm. Data points represent the two values expressed as number of cells. There was no significant correlation between the number of cells that entered meiosis (in a 10 hour EdU label) and the number of progenitor zone cells within day 1, 3, or 5 adults. n=18, 13, 9. Comparison by Pearson Correlation. (See Supplemental Table S8 for statistics)

Development • Supplementary information

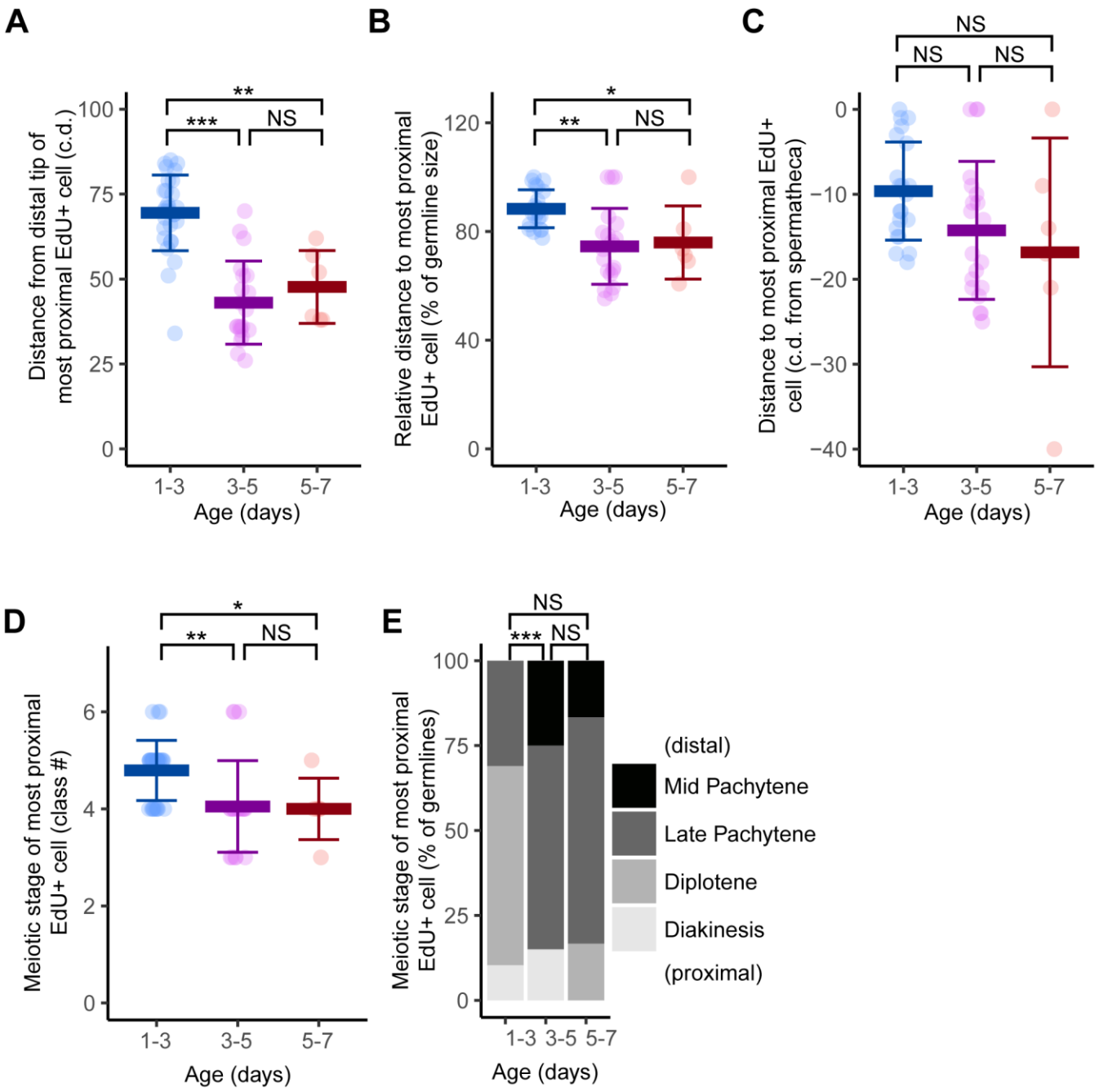


**Figure S9. Age-related decrease in the rate of meiotic progression**

Mated hermaphrodites at day 1 (blue), 3 (purple), or 5 (red) were exposed to EdU labeled bacteria for 4 hours ("pulse"), transferred to unlabeled bacteria for 48 hours ("chase"), and germlines were dissected and stained with anti-WAPL-1 antibody and EdU click chemistry. The most proximal EdU positive cells were identified, and their position and meiotic stage were determined.

**A)** Each data point indicates the distance from the distal tip of the gonad arm to the most proximal EdU positive cell in cell diameters.

Development • Supplementary information

**B)** Each data point indicates the distance from the distal tip of the gonad arm to the most proximal EdU positive cell, divided by the distance from the distal tip of the gonad arm to the spermatheca (size of the germline).
**C)** Each data point indicates the distance from the spermatheca to the most proximal EdU positive cell in cell diameters. We defined the position of the spermatheca as 0, and negative values indicate positions distal to the spermatheca. Comparison by Kruskal-Wallis test.
**D)** To facilitate statistical tests of an ordered categorical variable, we defined mid-pachytene = 3, late-pachytene = 4, diplotene = 5, and diakinesis = 6, similar to Jaramillo-Lambert et al., (2007). Each data point indicates the numeric meiotic stage of the most proximal EdU positive cell. Comparison by Kruskal-Wallis test.
**E)** In each germline, the most proximal EdU labeled cell was identified and categorized as mid pachytene, late pachytene, diplotene or diakinesis stage of meiosis. Comparison by Pearson's Chi-squared test. Only a small number of germlines were included in the day 5-7 data, which may contribute to the lack of significance in comparisons with that age (See Supplemental Table S9 for statistics).

Development • Supplementary information

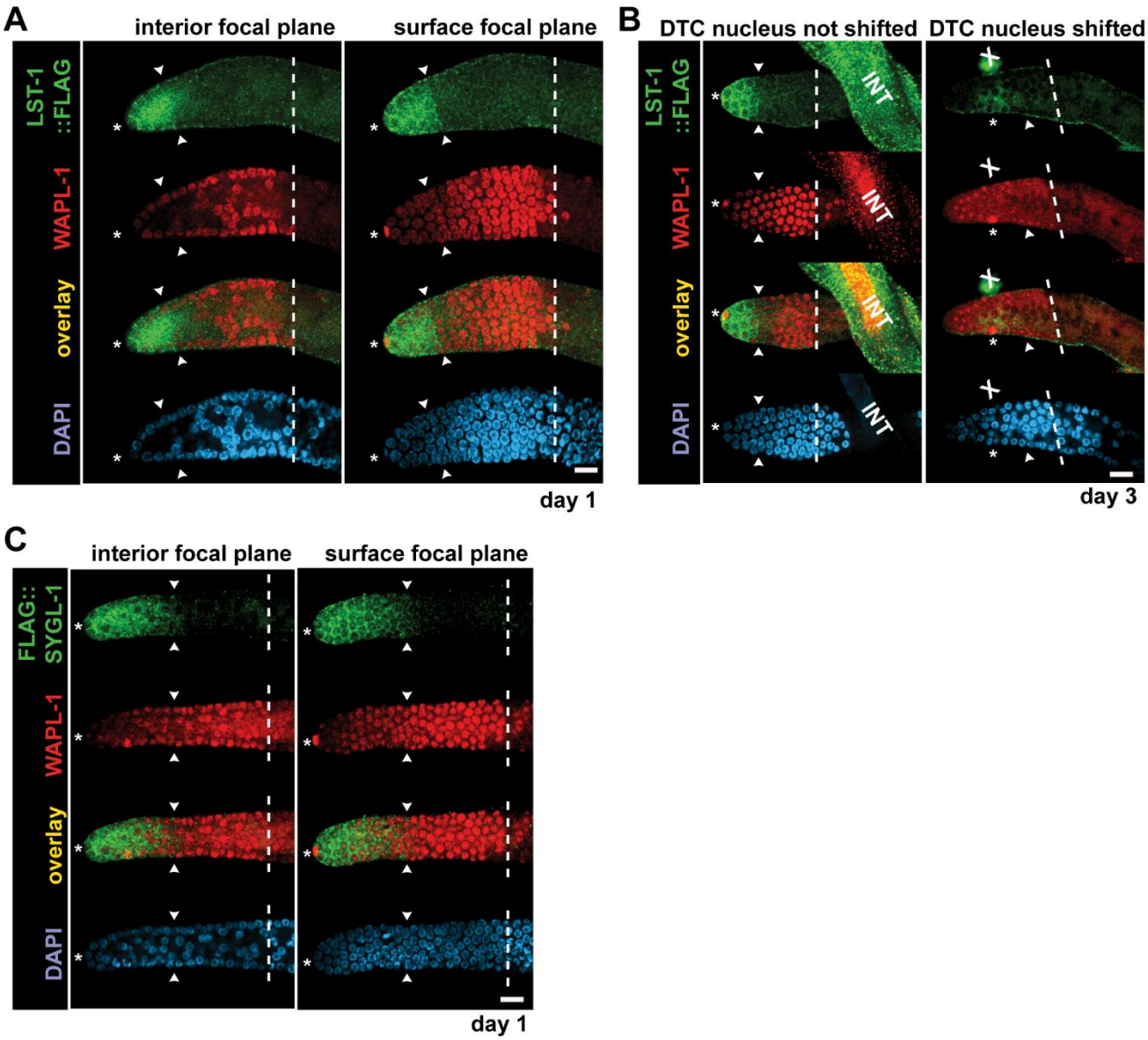


**Figure S10. Distribution of LST-1::FLAG and FLAG::SYGL-1 in the surface and interior of germlines and relative to the position of the DTC nucleus.**

**A-C)** Representative fluorescence microscope image of one germline stained for FLAG (green, row 1), WAPL-1 (red, row 2), FLAG and WAPL-1 (overlay, row 3) and DAPI (blue, row 4). Asterisk indicates the position of the DTC nucleus, white arrowheads indicate the proximal boundary of FLAG staining, and white dashed lines indicate the proximal boundary of WAPL-1-positive cells. Scale bar = 10 μm.

**A)** Day 1 germline with LST-1::FLAG. Panels on left display a focal plane from the interior of the germline, whereas panels on right display a focal plane from the surface of the germline.

**B)** Day 3 germlines with LST-1::FLAG. Panels on left show a germline with the DTC nucleus at position 1. Panels on right show a germline with the DTC nucleus shifted to position 6. Note that LST-1::FLAG signal is positioned near the shifted DTC nucleus, not near the distal tip of the germline. INT indicates intestine; X indicates a speck of green dust.

**C)** Day 1 germline with FLAG::SYGL-1. Panels on left display a focal plane from the interior of the germline, whereas panels on right display a focal plane from the surface of the germline.

Development • Supplementary information

**Table S1. Data for Figure 1: The female reproductive system displayed rapid age-related decline in sperm-replete *C. elegans***

[1] Adult days. L4 stage = day 0.

[2] Mean value rounded to whole number. View data in spreadsheet for decimal values.

[3] Standard deviation.

[4] Number of animals in experiment producing one or more viable egg during a 24-hour period. Some animals died of matricidal hatching or vulval extrusion and were censored from the experiment.

[5] Number of animals in experiment producing no viable eggs during a 24-hour period, that were alive with no evidence of internal hatching of embryos or vulval extrusion.

[6] Progeny production on a given day, divided by peak progeny production on day 2, expressed as percent.

[7] Sample size (number of P0 "mother" animals).

[8] ND = Not determined, as animals were mated in groups on day 1.

Click here to Download Table S1

**Table S2. Data for Figure 2: Endomitotic oocytes and a shifted DTC nucleus occurred at a low frequency**

[1] Summary of values, mean, standard deviation, and sample size (n). Sample size is expressed as the number of animals or germlines, as indicated. Mean and standard deviations rounded to whole number or one decimal. View data in spreadsheet for decimal values.

[2] Global comparisons were used to test overall differences between all groups.

[3] Post-hoc comparisons were used for pairwise tests and to correct for multiple comparisons (familywise error).

[4] Both parametric tests, which assume the data are normally distributed, and non-parametric tests were performed for all comparisons.

Click here to Download Table S2

**Table S3. Data for Figure 3: Population-wide, age-related decreases in the size of the germline and progenitor zone**

[1] Summary of values, mean, standard deviation, and sample size (n). Sample size is expressed as the number of animals or germlines, as indicated. Mean and standard deviations rounded to whole number or one decimal. View data in spreadsheet for decimal values.

[2] Global comparisons were used to test overall differences between all groups.

[3] Post-hoc comparisons were used for pairwise tests and to correct for multiple comparisons (familywise error).

[4] Both parametric tests, which assume the data are normally distributed, and non-parametric tests were performed for all comparisons.

Click here to Download Table S3

Development • Supplementary information

**Table S4. Data for Figure 4: An age-related increase in the duration of the cell cycle**

[1] Summary of values, mean, standard deviation, and sample size (n). Sample size is expressed as the number of animals or germlines, as indicated. Mean and standard deviations rounded to whole number or one decimal. View data in spreadsheet for decimal values.

[2] Global comparisons were used to test overall differences between all groups.

[3] Post-hoc comparisons were used for pairwise tests and to correct for multiple comparisons (familywise error).

[4] Both parametric tests, which assume the data are normally distributed, and non-parametric tests were performed for all comparisons.

Click here to Download Table S4

**Table S5. Data for Figure 5: Age-related decrease in the rate of meiotic entry**

[1] Summary of values, mean, standard deviation, and sample size (n). Sample size is expressed as the number of animals or germlines, as indicated. Mean and standard deviations rounded to whole number or one decimal. View data in spreadsheet for decimal values.

[2] Global comparisons were used to test overall differences between all groups.

[3] Post-hoc comparisons were used for pairwise tests and to correct for multiple comparisons (familywise error).

[4] Both parametric tests, which assume the data are normally distributed, and non-parametric tests were performed for all comparisons.

Click here to Download Table S5

**Table S6. Data for Figure 6: Age-related decrease in the rate of meiotic progression**

[1] Summary of values, mean, standard deviation, and sample size (n). Sample size is expressed as the number of animals or germlines, as indicated. Mean and standard deviations rounded to whole number or one decimal. View data in spreadsheet for decimal values.

[2] Global comparisons were used to test overall differences between all groups.

[3] Post-hoc comparisons were used for pairwise tests and to correct for multiple comparisons (familywise error).

[4] Both parametric tests, which assume the data are normally distributed, and non-parametric tests were performed for all comparisons.

Click here to Download Table S6

Development • Supplementary information

**Table S7. Data for Figure 7: Population-wide age-related decrease in the stem cell pool and GLP-1 (Notch) signaling**

[1] Summary of values, mean, standard deviation, and sample size (n). Sample size is expressed as the number of animals or germlines, as indicated. Mean and standard deviations rounded to whole number or one decimal. View data in spreadsheet for decimal values.

[2] Global comparisons were used to test overall differences between all groups.

[3] Post-hoc comparisons were used for pairwise tests and to correct for multiple comparisons (familywise error).

[4] Both parametric tests, which assume the data are normally distributed, and non-parametric tests were performed for all comparisons.

Click here to Download Table S7

**Table S3: Data for Supplemental Figure 3: Endomitotic oocytes and a shifted DTC nucleus occurred at a low frequency**

[1] Summary of values, mean, standard deviation, and sample size (n). Sample size is expressed as the number of animals or germlines, as indicated. Mean and standard deviations rounded to whole number or one decimal. View data in spreadsheet for decimal values.

[2] Global comparisons were used to test overall differences between all groups.

[3] Post-hoc comparisons were used for pairwise tests and to correct for multiple comparisons (familywise error).

[4] Both parametric tests, which assume the data are normally distributed, and non-parametric tests were performed for all comparisons.

[5] Intraclass correlation was used to compare the pooled variance between pairs of germlines from one animal and pooled variance within pairs. Pearson's interclass correlation was used to test for linear relationships between variables.

Click here to Download Table S3

Development • Supplementary information

**Table S4: Data for Supplemental Figure 4: Correlational analysis of distal phenotypes.**

[1] Summary of values, mean, standard deviation, and sample size (n). Sample size is expressed as the number of animals or germlines, as indicated. Mean and standard deviations rounded to whole number or one decimal. View data in spreadsheet for decimal values.
[2] Global comparisons were used to test overall differences between all groups.
[3] Post-hoc comparisons were used for pairwise tests and to correct for multiple comparisons (familywise error).
[4] Both parametric tests, which assume the data are normally distributed, and non-parametric tests were performed for all comparisons.
[5] Intraclass correlation was used to compare the pooled variance between pairs of germlines from one animal and pooled variance within pairs. Pearson's interclass correlation was used to test for linear relationships between variables.

Click here to Download Table S4

**Table S5: Data for Supplemental Figure 5: Effect of mating on germline size**

[1] Summary of values, mean, standard deviation, and sample size (n). Sample size is expressed as the number of animals or germlines, as indicated. Mean and standard deviations rounded to whole number or one decimal. View data in spreadsheet for decimal values.
[2] Global comparisons were used to test overall differences between all groups.
[3] Post-hoc comparisons were used for pairwise tests and to correct for multiple comparisons (familywise error).
[4] Both parametric tests, which assume the data are normally distributed, and non-parametric tests were performed for all comparisons.
[5] Intraclass correlation was used to compare the pooled variance between pairs of germlines from one animal and pooled variance within pairs. Pearson's interclass correlation was used to test for linear relationships between variables.

Click here to Download Table S5

Development • Supplementary information

**Table S6 : Data for Supplemental Figure 6: A fraction of day 5 animals displayed no EdU labeling**

[1] Summary of values, mean, standard deviation, and sample size (n). Sample size is expressed as the number of animals or germlines, as indicated. Mean and standard deviations rounded to whole number or one decimal. View data in spreadsheet for decimal values.
[2] Intraclass correlation was used to compare the pooled variance between pairs of germlines from one animal and pooled variance within pairs. Pearson's interclass correlation was used to test for linear relationships between variables.

Click here to Download Table S6

**Table S7: Data for Supplemental Figure 7: Age-related change in the numbers of M-phase and S-phase cells**

[1] Summary of values, mean, standard deviation, and sample size (n). Sample size is expressed as the number of animals or germlines, as indicated. Mean and standard deviations rounded to whole number or one decimal. View data in spreadsheet for decimal values.
[2] Global comparisons were used to test overall differences between all groups.
[3] Post-hoc comparisons were used for pairwise tests and to correct for multiple comparisons (familywise error).
[4] Both parametric tests, which assume the data are normally distributed, and non-parametric tests were performed for all comparisons.

Click here to Download Table S7

**Table S8: Data for Supplemental Figure 8: Age-related decrease in the rate of meiotic entry**

[1] Summary of values, mean, standard deviation, and sample size (n). Sample size is expressed as the number of animals or germlines, as indicated. Mean and standard deviations rounded to whole number or one decimal. View data in spreadsheet for decimal values.
[2] Global comparisons were used to test overall differences between all groups.
[3] Post-hoc comparisons were used for pairwise tests and to correct for multiple comparisons (familywise error).
[4] Both parametric tests, which assume the data are normally distributed, and non-parametric tests were performed for all comparisons.

Development • Supplementary information

[5] Intraclass correlation was used to compare the pooled variance between pairs of germlines from one animal and pooled variance within pairs. Pearson's interclass correlation was used to test for linear relationships between variables.
[6] Sample size only includes cells which entered meiosis.

Click here to Download Table S8

**Table S9: Data for Supplemental Figure 9: Age-related decrease in the rate of meiotic progression**

[1] Summary of values, mean, standard deviation, and sample size (n). Sample size is expressed as the number of animals or germlines, as indicated. Mean and standard deviations rounded to whole number or one decimal. View data in spreadsheet for decimal values.
[2] Global comparisons were used to test overall differences between all groups.
[3] Post-hoc comparisons were used for pairwise tests and to correct for multiple comparisons (familywise error).
[4] Both parametric tests, which assume the data are normally distributed, and non-parametric tests were performed for all comparisons.

Click here to Download Table S9

Development • Supplementary information